ARTICLE

https://doi.org/10.1038/s41586-018-0563-7

Plant functional trait change across a warming tundra biome

A list of authors and their affiliations appears online.

The tundra is warming more rapidly than any other biome on Earth, and the potential ramifications are far-reaching because of global feedback effects between vegetation and climate. A better understanding of how environmental factors shape plant structure and function is crucial for predicting the consequences of environmental change for ecosystem functioning. Here we explore the biome-wide relationships between temperature, moisture and seven key plant functional traits both across space and over three decades of warming at 117 tundra locations. Spatial temperature–trait relationships were generally strong but soil moisture had a marked influence on the strength and direction of these relationships, highlighting the potentially important influence of changes in water availability on future trait shifts in tundra plant communities. Community height increased with warming across all sites over the past three decades, but other traits lagged far behind predicted rates of change. Our findings highlight the challenge of using space-for-time substitution to predict the functional consequences of future warming and suggest that functions that are tied closely to plant height will experience the most rapid change. They also reveal the strength with which environmental factors shape biotic communities at the coldest extremes of the planet and will help to improve projections of functional changes in tundra ecosystems with climate warming.

Rapid climate warming in Arctic and alpine regions is driving changes in the structure and composition of tundra ecosystems[1,2], with potentially global consequences. Up to 50% of the world's belowground carbon stocks are contained in permafrost soils[3], and tundra regions are expected to contribute the majority of warming-induced soil carbon loss over the next century[4]. Plant traits strongly affect carbon cycling and the energy balance of the ecosystem, which can in turn influence regional and global climates[5–7]. Traits related to the resource economics spectrum[8], such as specific leaf area (SLA), leaf nitrogen content and leaf dry matter content (LDMC), affect primary productivity, litter decomposability, soil carbon storage and nutrient cycling[5,6,9,10], while size-related traits, such as leaf area and plant height, influence aboveground carbon storage, albedo (that is, surface reflectance) and hydrology[11–13] (Extended Data Table 1). Quantifying the link between the environment and plant functional traits is therefore important to understanding the consequences of climate change, but such studies rarely extend into the tundra[14–16]. Thus, the full extent of the relationship between climate and plant traits in the coldest ecosystems on Earth has yet to be assessed, and the consequences of climate warming for functional change in the tundra remain largely unknown.

Here we quantify the biome-wide relationships between temperature, soil moisture and key traits that represent the foundation of plant form and function[17], using a dataset of more than 56,000 tundra plant trait observations (Fig. 1a, Extended Data Fig. 1a and Supplementary Table 1). We examine five continuously distributed traits related to plant size (adult plant height and leaf area) and to resource economy (SLA, leaf nitrogen content and LDMC), as well as two categorical traits related to community-level structure (woodiness) and leaf phenology and lifespan (evergreenness). Intraspecific trait variability is thought to be especially important in regions where diversity is low or where species have wide geographical ranges[18], as in the tundra. Thus, we analyse two underlying components of biogeographical patterns in the five continuous traits: intraspecific variability (phenotypic plasticity or genetic differences among populations) and community-level variability (species turnover or shifts in the abundances of species across space). We first investigated how plant traits vary with temperature and soil moisture across the tundra biome. We then quantified the relative influence of intraspecific trait variation (ITV) versus community-level trait variation (estimated as community-weighted trait means (CWM)) for spatial temperature–trait relationships. Finally, we investigated whether spatial temperature–trait relationships are explained by among-site differences in species abundance or species turnover (presence or absence).

A major incentive for quantifying spatial temperature–trait relationships is to provide an empirical basis for predicting the potential consequences of future warming[19–21]. Thus, we also estimate realized rates of community-level trait change over time using nearly three decades of vegetation survey data at 117 tundra sites (Fig. 1a and Supplementary Table 2). Focusing on interspecific trait variation, we investigated how changes in community traits over three decades of ambient warming compare to predictions from spatial temperature–trait relationships. We expect greater temporal trait change when spatial temperature–trait relationships are (a) strong, (b) unlimited by moisture availability and (c) due primarily to abundance shifts instead of species turnover, given that species turnover over time depends on immigration and is likely to be slow[22]. Finally, because total realized trait change in continuous traits consists of both community-level variation and ITV, we estimated the potential contribution of ITV to overall trait change (CWM + ITV) using the modelled intraspecific temperature–trait relationships described above (see Methods and Extended Data Fig. 1b). For all analyses, we used a generalizable Bayesian modelling approach, which allowed us to account for the hierarchical spatial, temporal and taxonomic structure of the data as well as multiple sources of uncertainty.

Environment–trait relationships across the tundra biome

We found strong spatial associations between temperature and community height, SLA and LDMC (Fig. 2a, Extended Data Fig. 2 and Supplementary Table 3) across the 117 survey sites. Both height and SLA increased with summer temperature, but the temperature–trait relationship for SLA was much stronger at wetter than at drier sites. LDMC was negatively related to temperature, and

© 2018 Springer Nature Limited. All rights reserved.

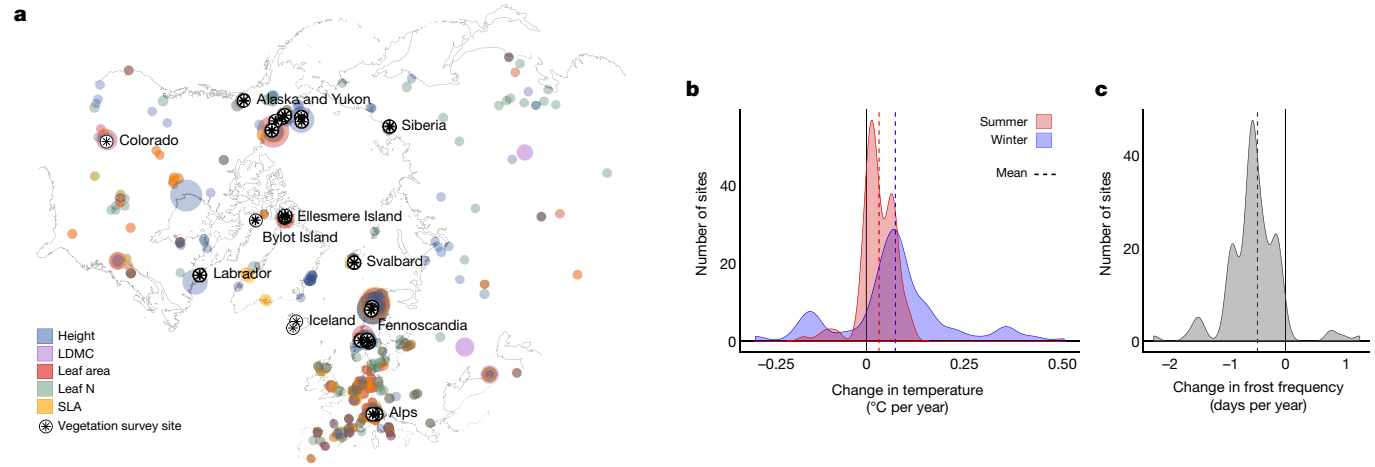

Fig. 1 | Geographical distribution of trait and vegetation survey data and climatic change over the study period. a, Map of all 56,048 tundra trait records and 117 vegetation survey sites. **b**, **c**, Climatic change across the period of monitoring at the 117 vegetation survey sites, represented as mean winter (coldest quarter) and summer (warmest quarter) temperature (**b**) and frost day frequency (**c**). The size of the coloured points on the map indicates the relative quantity of trait measurements (larger circles indicate more measurements of that trait at a given location) and the colour indicates which trait was measured. The black stars indicate the vegetation survey sites used in the community trait analyses (most stars represent multiple sites). Trait data were included for all species that occurred in at least one tundra vegetation survey site; thus, although not all species are unique to the tundra, all do occur in the tundra. Temperature change and frost frequency change were estimated for the interval over which sampling was conducted at each site plus the preceding four years, to best reflect the time window over which tundra plant communities respond to temperature change[20,29].

more strongly so at wetter than drier sites. Community woodiness decreased with temperature, but the ratio of evergreen to deciduous woody species increased with temperature, particularly at drier sites (Extended Data Fig. 3). These spatial temperature–trait relationships indicate that long-term climate warming should cause pronounced shifts towards communities of taller plants with more resource-acquisitive leaves (high SLA and low LDMC), particularly where soil moisture is high.

Our results reveal a substantial moderating influence of soil moisture on community traits across spatial temperature gradients[2,23]. Both leaf area and leaf nitrogen content decreased with warmer temperatures in dry sites but increased with warmer temperatures in wet sites (Fig. 2a and Supplementary Table 4). Soil moisture was important for explaining spatial variation in all seven investigated traits, even when temperature alone was not (for example, leaf area; Fig. 2a and Extended Data Fig. 2), potentially reflecting physiological constraints that are related to heat exchange or frost tolerance when water availability is low[24]. Thus, future warming-driven changes in traits and associated ecosystem functions (for example, decomposability) will probably depend on current soil moisture conditions at a site[23]. Furthermore, future changes in water availability (for example, because of changes in precipitation, snow melt timing, permafrost and hydrology[25]) could cause substantial shifts in these traits and their associated functions, irrespective of warming.

We found consistent intraspecific temperature–trait relationships for all five continuous traits (Fig. 2b and Supplementary Table 5). Intraspecific plant height and leaf area showed strong positive relationships with summer temperature (that is, individuals were taller and had larger leaves in warmer locations), whereas intraspecific LDMC, leaf nitrogen content and SLA were related to winter but not summer temperature (Extended Data Fig. 2). The differences in responses of ITV to summer versus winter temperatures may indicate that size-related traits better reflect summer growth potential, whereas resource-economics traits reflect tolerance to cold-stress. These results, although correlative, indicate that trait variation expressed at the individual or population level is related to the growing environment and that warming will probably lead to substantial intraspecific change in many traits. Thus, the potential for trait change over time is underestimated by using species-level trait means alone. Future work is needed to disentangle the role of plasticity and genetic differentiation in explaining the observed intraspecific temperature–trait relationships[26], as this will also influence the rate of future trait change[27]. Trait measurements collected over time and under novel (experimental) conditions, as yet unavailable, would enable more accurate predictions of future intraspecific trait change.

Partitioning the underlying causes of community temperature–trait relationships revealed that species turnover explained most of the variation in traits across space (Fig. 2c), suggesting that dispersal and immigration processes will primarily govern the rate of ecosystem responses to warming. Shifts in the abundances of species and ITV accounted for a relatively small part of the overall temperature–trait relationship across space (Fig. 2c). Furthermore, the local trait pool in the coldest tundra sites (mean summer temperature $<3\,°C$) is constrained relative to the tundra as a whole for many traits (Extended Data Fig. 4). Together, these results indicate that the magnitude of warming-induced community trait shifts will be limited without the arrival of novel species from warmer environments.

Change in community traits over time

Plant height was the only trait for which the CWM changed over the 27 years of monitoring; it increased rapidly at nearly every survey site (Fig. 3a, b, Extended Data Fig. 3 and Supplementary Table 6). Interannual variation in community height was sensitive to summer temperature (Fig. 3c, Extended Data Fig. 2 and Supplementary Table 7), indicating that increases in community height are responding to warming. However, neither the total rate of temperature change nor soil moisture predicted the total rate of CWM change in any trait (Extended Data Fig. 5 and Supplementary Table 8). Incorporating potential ITV doubled the average estimate of plant height change over time (Figs. 3a, 4a, dashed lines). Because spatial patterns in ITV can be due to both phenotypic plasticity and genetic differences among populations, this is likely to be a maximum estimate of the ITV contribution to trait change (for example, if intraspecific temperature–trait relationships are due entirely to phenotypic plasticity). The observed increase in community height is consistent with previous findings of increasing vegetation height in response to experimental warming at a subset of these sites[28] and with studies showing increased shrub growth over time[11].

© 2018 Springer Nature Limited. All rights reserved.

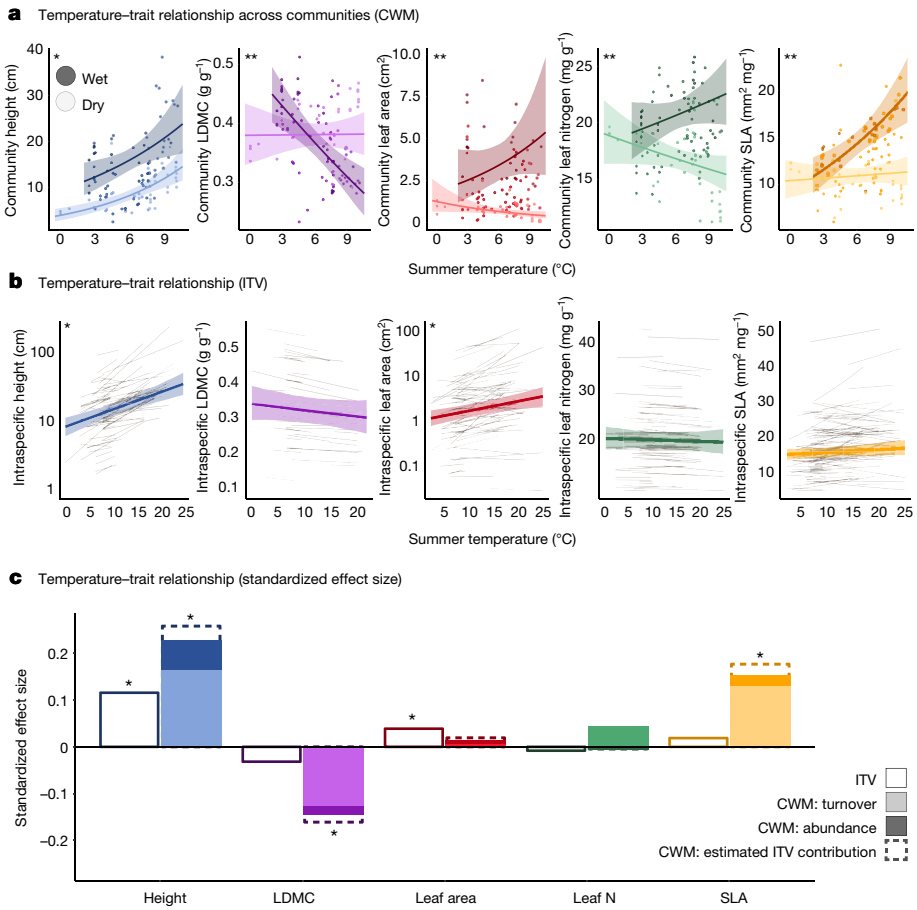

Fig. 2 | Strong spatial relationships in traits across temperature and soil moisture gradients are primarily explained by species turnover. **a**, Spatial relationship between community-level (CWM) functional traits, mean summer (warmest quarter) temperature and soil moisture ($n = 1{,}520$ plots within 117 sites within 72 regions). **b**, Spatial relationship between summer temperature and ITV (note the log scale for height and leaf area). **c**, Standardized effect sizes were estimated for all temperature–trait relationships both across communities (CWM; solid bars) and within species (ITV; open bars with solid outlines). Effect sizes for CWM temperature–trait relationships were further partitioned into the proportion of the effect driven solely by species turnover (light bars) and abundance shifts (dark bars) over space. Dashed lines indicate the estimated additional contribution of ITV to the total temperature–trait relationship (CWM + ITV). The contribution of ITV is estimated from the spatial temperature–trait relationships modelled in **b**. Soil moisture in **a** was modelled as continuous but is shown predicted only at low and high values to improve visualization. Transparent ribbons in **a** and **b** indicate 95% credible intervals for model mean predictions. Grey lines in **b** represent intraspecific temperature–trait relationships for each species (height, $n = 80$ species; LDMC, $n = 43$; leaf area, $n = 85$; leaf nitrogen content (leaf N), $n = 85$; SLA, $n = 108$; the number of observations per trait is shown in Supplementary Table 1). In all panels, asterisks indicate that the 95% credible interval on the slope of the temperature–trait relationship did not overlap zero. In **a**, two asterisks indicate that the temperature × soil moisture interaction term did not overlap zero. Winter temperature–trait relationships are shown in Extended Data Fig. 2. Community woodiness and evergreenness are shown in Extended Data Fig. 3.

Increasing community height over time was mostly attributable to species turnover (rather than shifts in abundance of the resident species; Fig. 3b) and was driven by the immigration of taller species rather than the loss of shorter ones (Extended Data Fig. 6 and Supplementary Table 9). This turnover could reflect the movement of tall species upward in latitude and elevation or from local species pools in nearby warmer microclimates. The magnitude of temporal change was comparable to the change predicted based on the spatial temperature–trait relationship (Fig. 4a, solid lines), indicating that temporal change in plant height is not currently limited by immigration rates. The importance of immigration in explaining changes in community height is surprising given the relatively short study duration and long lifespan of tundra plants, but is nonetheless consistent with a previous finding of shifts towards warm-associated species in tundra plant communities[20,29]. If the observed rate of trait change continues (for example, if immigration were unlimited), community height (excluding potential change due to ITV) could increase by 20–60% by the end of the century, depending on carbon emission, warming and water availability scenarios (Extended Data Fig. 7).

Consequences and implications

Recent (observed) and future (predicted) changes in plant traits, particularly height, are likely to have important implications for ecosystem functions and feedback effects involving soil temperature[30,31], decomposition[5,10] and carbon cycling[32], as the potential for soil carbon loss is particularly great in high-latitude regions[4]. For example, increasing plant height could offset warming-driven carbon loss through increased carbon storage due to woody litter production[5] or through reduced decomposition owing to lower summer soil temperatures caused by shading[3,30,32] (negative feedback effects). Positive feedback effects are also possible if branches or leaves above the snowpack reduce albedo[11,12] or increase snow accumulation, leading to warmer soil temperatures in winter and increased decomposition rates[3,11]. The balance of these feedback systems—and thus the net effect of trait change on carbon cycling—may depend on the interaction between warming and changes in snow distribution[33] and water availability[34], which remain mostly unknown for the tundra biome.

The lack of an observed temporal trend in SLA and LDMC, despite strong temperature–trait relationships over space, highlights the limitations of using space-for-time substitution for predicting

© 2018 Springer Nature Limited. All rights reserved.

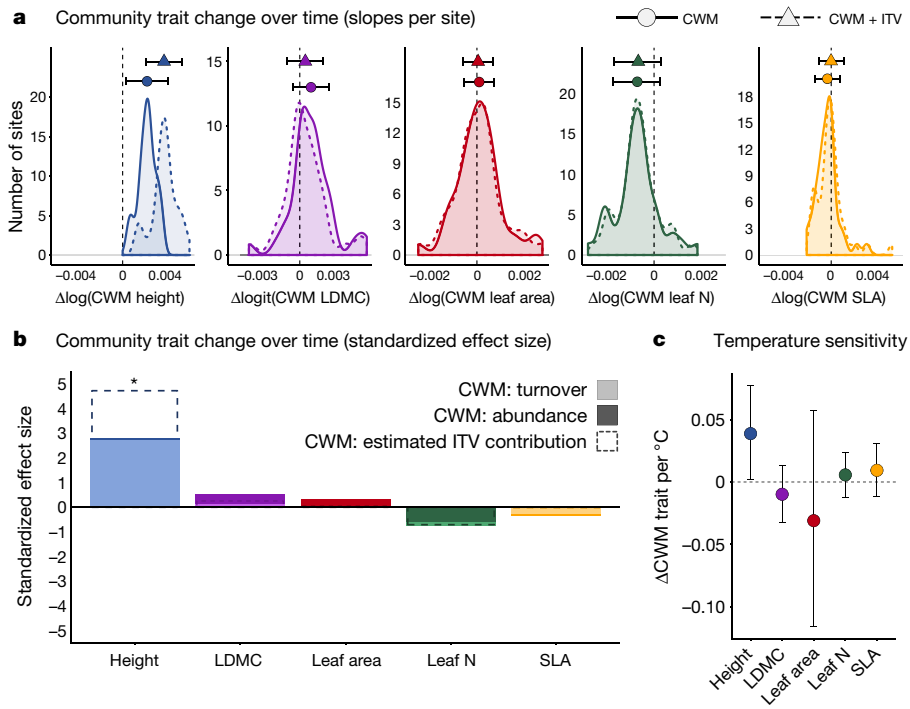

Fig. 3 | A tundra-wide increase in community height over time is related to warming. a, Observed community trait change per year (transformed units). Solid lines indicate the distribution of CWM model slopes (trait change per site) whereas dashed lines indicate change in CWM plus potential intraspecific change modelled from spatial temperature–trait relationships (CWM + ITV). Circles (CWM) or triangles (CWM + ITV) and error bars indicate the mean and 95% credible interval for the overall rate of trait change across all sites ($n = 4{,}575$ plot-years within 117 sites within 38 regions). The vertical black dashed line indicates 0 (no change over time). **b**, Standardized effect sizes for CWM change over time were further partitioned into the proportion of the effect driven solely by species turnover (light bars) or shifts in abundance of resident species (dark bars) over time. Dashed lines indicate the estimated additional contribution of ITV to total trait change over time (CWM + ITV). Asterisks indicate that the 95% credible interval on the mean hyperparameter for CWM trait change over time did not overlap zero. **c**, Temperature sensitivity of each trait (that is, correspondence between interannual variation in CWM trait values and interannual variation in summer temperature). Temperatures associated with each survey year were estimated as five-year means (temperature of the survey year and four preceding years), because this interval has been shown to be most relevant to vegetation change in tundra[20] and alpine[29] plant communities. Circles represent the mean temperature sensitivity across all 117 sites, error bars are 95% credible intervals on the mean. Changes in community woodiness and evergreenness are shown in Extended Data Fig. 3.

short-term ecological change. This disconnect could reflect the influence of unmeasured changes in water availability (for example, owing to local-scale variation in the timing of snowmelt or hydrology) that counter or overwhelm the effect of static soil moisture estimates. For example, we would not expect substantial changes in traits demonstrating a spatial temperature × moisture interaction (LDMC, leaf area, leaf nitrogen content and SLA), even in wet sites, if warming also leads to drier soils. Plant height was the only continuous trait for which a temperature × moisture interaction was not important, and was predicted to increase across all areas of the tundra regardless of recent soil moisture trends (Fig. 4c, d). Spatiotemporal disconnects could also reflect dispersal limitation of potential immigrants (for example, with low LDMC and high SLA) or establishment failure due to novel biotic[35] or abiotic[36] conditions other than temperature to which immigrants are maladapted[22,36]. Furthermore, community responses to climate warming could be constrained by soil properties (for example, organic matter and mineralization) that themselves respond slowly to warming[20].

The patterns in functional traits described here reveal the extent to which environmental factors shape biotic communities in the tundra. Strong temperature- and moisture-related spatial gradients in traits related to competitive ability (for example, height) and resource capture and retention (for example, leaf nitrogen and SLA) reflect trade-offs in plant ecological strategy[9,37] from benign (warm, wet) to extreme (cold, dry) conditions. Community-level trait syndromes, as reflected in ordination axes, are also strongly related to both temperature and moisture, suggesting that environmental drivers structure not only individual traits but also trait combinations—and thus lead to a limited number of successful functional strategies in some environments (for example, woody, low-SLA and low-leaf nitrogen communities in warm, dry sites; Extended Data Fig. 8). Thus, warming may lead to a community-level shift towards more acquisitive plant strategies[37] in wet tundra sites, but towards more conservative strategies in drier sites as moisture becomes more limiting.

Earth system models are increasingly moving to incorporate relationships between traits and the environment, as this can substantially improve estimates of ecosystem change[38–40]. Our results inform these projections of future tundra functional change[38] by explicitly quantifying the link between temperature, moisture and key functional traits across the biome. In particular, our study highlights the importance of accounting for future changes in water availability, as this will probably influence both the magnitude and direction of change for many traits. In addition, we demonstrate that spatial trait–environment relationships are driven largely by species turnover, suggesting that modelling efforts must account for rates of species immigration when predicting the speed of future functional shifts. The failure of many traits (for example, SLA) to match expected rates of change suggests that space-for-time substitution alone may inaccurately represent near-term ecosystem change. Nevertheless, the ubiquitous increase in community plant height reveals that functional change is already occurring in tundra ecosystems.

Online content

Any methods, additional references, Nature Research reporting summaries, source data, statements of data availability and associated accession codes are available at https://doi.org/10.1038/s41586-018-0563-7.

© 2018 Springer Nature Limited. All rights reserved.

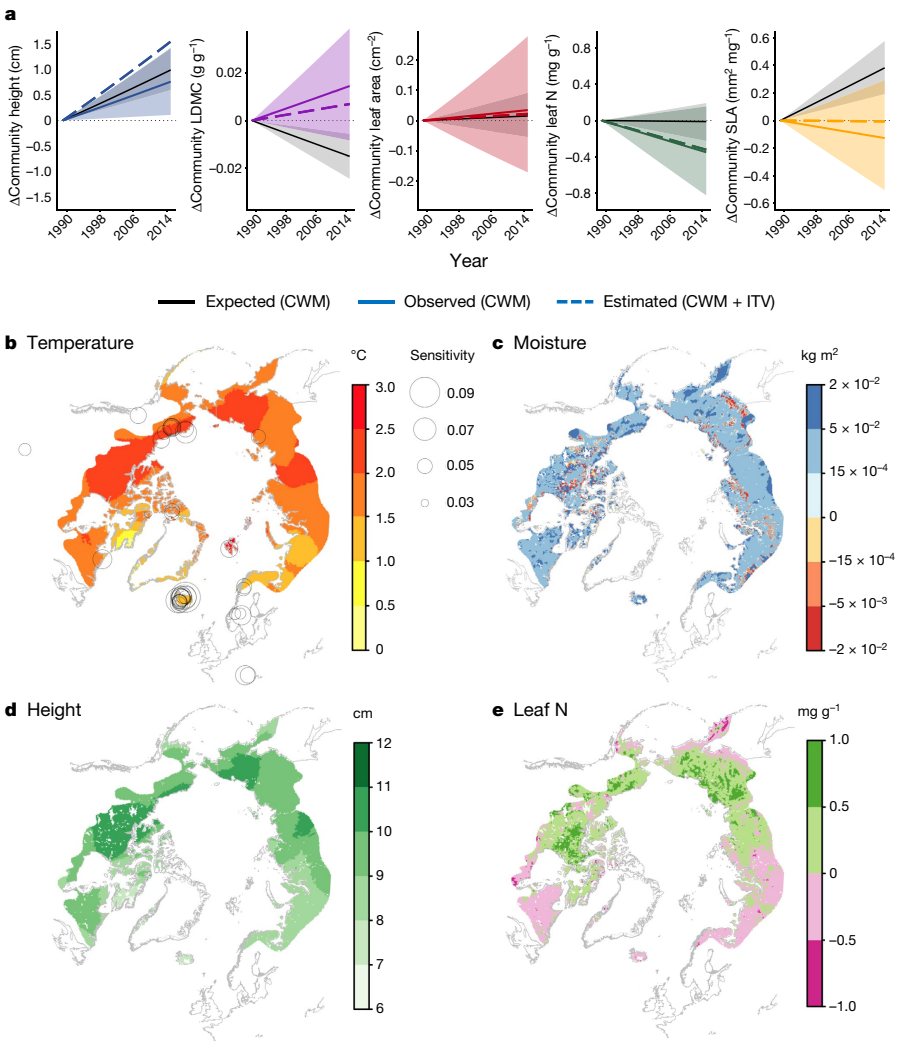

Fig. 4 | Community height increases in line with space-for-time predictions but other traits lag. a, Observed community (CWM) trait change over time (coloured lines) across all 117 sites versus expected CWM change over the duration of vegetation monitoring (1989–2015) based on the spatial temperature–trait (CWM) relationship and the average rate of recent summer warming across all sites (solid black lines). Coloured dashed lines indicate the estimated total change over time if predicted intraspecific trait variability is also included (CWM + ITV). Values on the *y* axis represent the magnitude of change relative to 0 (that is, trait anomaly), with 0 representing the trait value at t_0. **b**, **c**, Total recent temperature change (**b**) and soil moisture change (**c**) across the Arctic tundra (1979–2016). Temperature change estimates are derived from gridded temperature data from the Climate Research Unit (CRU), estimates of changes in soil moisture are derived from downscaled European Centre for Medium-Range Weather Forecasts Re-Analysis (ERA-Interim) soil moisture data. Circles in **b** represent the sensitivity (cm per °C) of CWM plant height to summer temperature at each site (see Fig. 3c). Areas of high temperature sensitivity are expected to experience the greatest increases in height with warming. **d**, **e**, Spatial trait–temperature–moisture relationships (Fig. 2a) were used to predict total changes in height (**d**) and leaf nitrogen content (**e**) over the entire 1979–2016 period based on concurrent changes in temperature and soil moisture. Note that **d** and **e** reflect the magnitude of expected change between 1979 and 2016, not observed trait change. See Methods for details on estimates of the change in temperature and soil moisture. The outline of Arctic areas is based on the Circumpolar Arctic Vegetation Map (http://www.geobotany.uaf.edu/cavm).

Received: 15 September 2017; Accepted: 8 August 2018;
Published online 26 September 2018.

1. Post, E. et al. Ecological dynamics across the Arctic associated with recent climate change. *Science* **325**, 1355–1358 (2009).
2. Elmendorf, S. C. et al. Plot-scale evidence of tundra vegetation change and links to recent summer warming. *Nat. Clim. Change* **2**, 453–457 (2012).
3. Sistla, S. A. et al. Long-term warming restructures Arctic tundra without changing net soil carbon storage. *Nature* **497**, 615–618 (2013).
4. Crowther, T. W. et al. Quantifying global soil carbon losses in response to warming. *Nature* **540**, 104–108 (2016).
5. Cornelissen, J. H. C. et al. Global negative vegetation feedback to climate warming responses of leaf litter decomposition rates in cold biomes. *Ecol. Lett.* **10**, 619–627 (2007).
6. Lavorel, S. & Garnier, E. Predicting changes in community composition and ecosystem functioning from plant traits: revisiting the Holy Grail. *Funct. Ecol.* **16**, 545–556 (2002).
7. Pearson, R. G. et al. Shifts in Arctic vegetation and associated feedbacks under climate change. *Nat. Clim. Change* **3**, 673–677 (2013).
8. Wright, I. J. et al. The worldwide leaf economics spectrum. *Nature* **428**, 821–827 (2004).
9. Díaz, S. et al. The plant traits that drive ecosystems: evidence from three continents. *J. Veg. Sci.* **15**, 295–304 (2004).
10. Cornwell, W. K. et al. Plant species traits are the predominant control on litter decomposition rates within biomes worldwide. *Ecol. Lett.* **11**, 1065–1071 (2008).
11. Myers-Smith, I. H. et al. Shrub expansion in tundra ecosystems: dynamics, impacts and research priorities. *Environ. Res. Lett.* **6**, 045509 (2011).
12. Sturm, M. & Douglas, T. Changing snow and shrub conditions affect albedo with global implications. *J. Geophys. Res.* **110**, G01004 (2005).
13. Callaghan, T. V. et al. Effects on the function of Arctic ecosystems in the short- and long-term perspectives. *Ambio* **33**, 448–458 (2004).
14. Moles, A. T. et al. Global patterns in plant height. *J. Ecol.* **97**, 923–932 (2009).
15. Moles, A. T. et al. Global patterns in seed size. *Glob. Ecol. Biogeogr.* **16**, 109–116 (2007).

© 2018 Springer Nature Limited. All rights reserved.

16. Reich, P. B. & Oleksyn, J. Global patterns of plant leaf N and P in relation to temperature and latitude. *Proc. Natl Acad. Sci. USA* **101**, 11001–11006 (2004).
17. Díaz, S. et al. The global spectrum of plant form and function. *Nature* **529**, 167–171 (2016).
18. Siefert, A. et al. A global meta-analysis of the relative extent of intraspecific trait variation in plant communities. *Ecol. Lett.* **18**, 1406–1419 (2015).
19. McMahon, S. M. et al. Improving assessment and modelling of climate change impacts on global terrestrial biodiversity. *Trends Ecol. Evol.* **26**, 249–259 (2011).
20. Elmendorf, S. C. et al. Experiment, monitoring, and gradient methods used to infer climate change effects on plant communities yield consistent patterns. *Proc. Natl Acad. Sci. USA* **112**, 448–452 (2015).
21. De Frenne, P. et al. Latitudinal gradients as natural laboratories to infer species' responses to temperature. *J. Ecol.* **101**, 784–795 (2013).
22. Sandel, B. et al. Contrasting trait responses in plant communities to experimental and geographic variation in precipitation. *New Phytol.* **188**, 565–575 (2010).
23. Ackerman, D., Griffin, D., Hobbie, S. E. & Finlay, J. C. Arctic shrub growth trajectories differ across soil moisture levels. *Glob. Change Biol.* **23**, 4294–4302 (2017).
24. Wright, I. J. et al. Global climatic drivers of leaf size. *Science* **357**, 917–921 (2017).
25. Wrona, F. J. et al. Transitions in Arctic ecosystems: ecological implications of a changing hydrological regime. *J. Geophys. Res. Biogeosci.* **121**, 650–674 (2016).
26. Read, Q. D., Moorhead, L. C., Swenson, N. G., Bailey, J. K. & Sanders, N. J. Convergent effects of elevation on functional leaf traits within and among species. *Funct. Ecol.* **28**, 37–45 (2014).
27. Albert, C. H., Grassein, F., Schurr, F. M., Vieilledent, G. & Violle, C. When and how should intraspecific variability be considered in trait-based plant ecology? *Perspect. Plant Ecol. Evol. Syst.* **13**, 217–225 (2011).
28. Elmendorf, S. C. et al. Global assessment of experimental climate warming on tundra vegetation: heterogeneity over space and time. *Ecol. Lett.* **15**, 164–175 (2012).
29. Gottfried, M. et al. Continent-wide response of mountain vegetation to climate change. *Nat. Clim. Change* **2**, 111–115 (2012).
30. Blok, D. et al. Shrub expansion may reduce summer permafrost thaw in Siberian tundra. *Glob. Change Biol.* **16**, 1296–1305 (2010).
31. Blok, D., Elberling, B. & Michelsen, A. Initial stages of tundra shrub litter decomposition may be accelerated by deeper winter snow but slowed down by spring warming. *Ecosystems* **19**, 155–169 (2016).
32. Cahoon, S. M. P. et al. Interactions among shrub cover and the soil microclimate may determine future Arctic carbon budgets. *Ecol. Lett.* **15**, 1415–1422 (2012).
33. Lawrence, D. M. & Swenson, S. C. Permafrost response to increasing Arctic shrub abundance depends on the relative influence of shrubs on local soil cooling versus large-scale climate warming. *Environ. Res. Lett.* **6**, 045504 (2011).
34. Christiansen, C. T. et al. Enhanced summer warming reduces fungal decomposer diversity and litter mass loss more strongly in dry than in wet tundra. *Glob. Change Biol.* **23**, 406–420 (2017).
35. Kaarlejärvi, E., Eskelinen, A. & Olofsson, J. Herbivores rescue diversity in warming tundra by modulating trait-dependent species losses and gains. *Nat Commun.* **8**, 419 (2017).
36. Bjorkman, A. D., Vellend, M., Frei, E. R. & Henry, G. H. R. Climate adaptation is not enough: warming does not facilitate success of southern tundra plant populations in the high Arctic. *Glob. Change Biol.* **23**, 1540–1551 (2017).
37. Reich, P. B. The world-wide 'fast–slow' plant economics spectrum: a traits manifesto. *J. Ecol.* **102**, 275–301 (2014).
38. Wullschleger, S. D. et al. Plant functional types in Earth system models: past experiences and future directions for application of dynamic vegetation models in high-latitude ecosystems. *Ann. Bot.* **114**, 1–16 (2014).
39. Butler, E. E. et al. Mapping local and global variability in plant trait distributions. *Proc. Natl Acad. Sci. USA* **114**, E10937–E10946 (2017).
40. Reich, P. B., Rich, R. L., Lu, X., Wang, Y.-P. & Oleksyn, J. Biogeographic variation in evergreen conifer needle longevity and impacts on boreal forest carbon cycle projections. *Proc. Natl Acad. Sci. USA* **111**, 13703–13708 (2014).

Acknowledgements This paper is an outcome of the sTundra working group supported by sDiv, the Synthesis Centre of the German Centre for Integrative Biodiversity Research (iDiv) Halle-Jena-Leipzig (DFG FZT 118). A.D.B. was supported by an iDiv postdoctoral fellowship and The Danish Council for Independent Research - Natural Sciences (DFF 4181-00565 to S.N.). A.D.B., I.H.M.-S., H.J.D.T. and S.A.-B. were funded by the UK Natural Environment Research Council (ShrubTundra Project NE/M016323/1 to I.H.M.-S.). S.N., A.B.O., S.S.N. and U.A.T. were supported by the Villum Foundation's Young Investigator Programme (VKR023456 to S.N.) and the Carlsberg Foundation (2013-01-0825). N.R. was supported by the DFG-Forschungszentrum 'German Centre for Integrative Biodiversity Research (iDiv) Halle-Jena-Leipzig' and Deutsche Forschungsgemeinschaft DFG (RU 1536/3-1). A.Buc. was supported by EU-F7P INTERACT (262693) and MOBILITY PLUS (1072/MOB/2013/0). A.B.O. was additionally supported by the Danish Council for Independent Research - Natural Sciences (DFF 4181-00565 to S.N.). J.M.A. was supported by the Carl Tryggers stiftelse för vetenskaplig forskning, A.H. by the Research Council of Norway (244557/E50), B.E. and A.Mic. by the Danish National Research Foundation (CENPERM DNRF100), B.M. by the Soil Conservation Service of Iceland and E.R.F. by the Swiss National Science Foundation (155554). B.C.F. was supported by the Academy of Finland (256991) and JPI Climate (291581). B.J.E. was supported by an NSF ATB, CAREER and Macrosystems award. C.M.I. was supported by the Office of Biological and Environmental Research in the US Department of Energy's Office of Science as part of the Next-Generation Ecosystem Experiments in the Arctic (NGEE Arctic) project. D.B. was supported by The Swedish Research Council (2015-00465) and Marie Skłodowska Curie Actions co-funding (INCA 600398). E.W. was supported by the National Science Foundation (DEB-0415383), UWEC–ORSP and UWEC–BCDT. G.S.-S. and M.I.-G. were supported by the University of Zurich Research Priority Program on Global Change and Biodiversity. H.D.A. was supported by NSF PLR (1623764, 1304040). I.S.J. was supported by the Icelandic Research Fund (70255021) and the University of Iceland Research Fund. J.D.M.S. was supported by the Research Council of Norway (262064). J.S.P. was supported by the US Fish and Wildlife Service. J.C.O. was supported by Klimaat voor ruimte, Dutch national research program Climate Change and Spatial Planning. J.F.J., P.G., G.H.R.H., E.L., N.B.-L., K.A.H., L.S.C. and T.Z. were supported by the Natural Sciences and Engineering Research Council of Canada (NSERC). G.H.R.H., N.B.-L., E.L., L.S.C. and L.H. were supported by ArcticNet. G.H.R.H., N.B.-L., M.Tr. and L.S.C. were supported by the Northern Scientific Training Program. G.H.R.H., E.L. and N.B.-L. were additionally supported by the Polar Continental Shelf Program. N.B.-L. was additionally supported by the Fonds de recherche du Quebec: Nature et Technologies and the Centre d'études Nordiques. J.P. was supported by the European Research Council Synergy grant SyG-2013-610028 IMBALANCE-P. A.A.-R., O.G. and J.M.N. were supported by the Spanish OAPN (project 534S/2012) and European INTERACT project (262693 Transnational Access). K.D.T. was supported by NSF ANS-1418123. L.E.S. and P.A.W. were supported by the UK Natural Environment Research Council Arctic Terrestrial Ecology Special Topic Programme and Arctic Programme (NE/K000284/1 to P.A.W.). P.A.W. was additionally supported by the European Union Fourth Environment and Climate Framework Programme (Project Number ENV4-CT970586). M.W. was supported by DFG RTG 2010. R.D.H. was supported by the US National Science Foundation. M.J.S. and K.N.S. were supported by the Niwot Ridge LTER (NSF DEB-1637686). H.J.D.T. was funded by a NERC doctoral training partnership grant (NE/L002558/1). V.G.O. was supported by the Russian Science Foundation (14-50-00029). L.B. was supported by NSF ANS (1661723) and S.J.G. by NASA ABoVE (NNX15AU03A/NNX17AE44G). B.B.-L. was supported as part of the Energy Exascale Earth System Model (E3SM) project, funded by the US Department of Energy, Office of Science, Office of Biological and Environmental Research. A.E. was supported by the Academy of Finland (projects 253385 and 297191). E.K. was supported by Swedish Research Council (2015-00498), and S.Dí. was supported by CONICET, FONCyT and SECyT-UNC, Argentina. The study has been supported by the TRY initiative on plant traits (http://www.try-db.org), which is hosted at the Max Planck Institute for Biogeochemistry, Jena, Germany and is currently supported by DIVERSITAS/Future Earth and the German Centre for Integrative Biodiversity Research (iDiv) Halle-Jena-Leipzig. A.D.B. and S.C.E. thank the US National Science Foundation for support to receive training in Bayesian methods (grant 1145200 to N. Thompson Hobbs). We thank H. Bruelheide and J. Ramirez-Villegas for helpful input at earlier stages of this project. We acknowledge the contributions of S. Mamet, M. Jean, K. Allen, N. Young, J. Lowe, O. Eriksson and many others to trait and community composition data collection, and thank the governments, parks, field stations and local and indigenous people for the opportunity to conduct research on their land.

Reviewer information *Nature* thanks G. Kunstler, F. Schrodt and the other anonymous reviewer(s) for their contribution to the peer review of this work.

Author contributions A.D.B., I.H.M.-S. and S.C.E. conceived the study, with input from the sTundra working group (S.N., N.R., P.S.A.B., A.B.-O., D.B., J.H.C.C., W.C., B.C.F., D.G., S.J.G., K.G., G.H.R.H., R.D.H., J.K., J.S.P., J.H.R.L., C.R., G.S.-S., H.J.D.T., M.V., M.W. and S.Wi.). A.D.B. performed the analyses, with input from I.H.M.-S., N.R., S.C.E. and S.N. D.N.K. made the maps of temperature, moisture and trait change. A.D.B. wrote the manuscript, with input from I.H.M.-S., S.C.E., S.N., N.R. and contributions from all authors. A.D.B. compiled the Tundra Trait Team database, with assistance from I.H.M.-S., H.J.D.T. and S.A.-B. Authorship order was determined as follows: (1) core authors; (2) sTundra participants (alphabetical) and other major contributors; (3) authors contributing both trait (Tundra Trait Team) and community composition (for example, ITEX) data (alphabetical); (4) Tundra Trait Team contributors (alphabetical); (5) contributors who provided community composition data only (alphabetical) and (6) contributors who provided TRY trait data (alphabetical).

Competing interests The authors declare no competing interests.

Additional information
Extended data is available for this paper at https://doi.org/10.1038/s41586-018-0563-7.
Supplementary information is available for this paper at https://doi.org/10.1038/s41586-018-0563-7.
Reprints and permissions information is available at http://www.nature.com/reprints.
Correspondence and requests for materials should be addressed to A.D.B.
Publisher's note: Springer Nature remains neutral with regard to jurisdictional claims in published maps and institutional affiliations.

© 2018 Springer Nature Limited. All rights reserved.

Anne D. Bjorkman[1,2,3]*, Isla H. Myers-Smith[1], Sarah C. Elmendorf[4,5,6], Signe Normand[2,7,8], Nadja Rüger[9,10], Pieter S. A. Beck[11], Anne Blach-Overgaard[2,8], Daan Blok[12], J. Hans C. Cornelissen[13], Bruce C. Forbes[14], Damien Georges[1,15], Scott J. Goetz[16], Kevin C. Guay[17], Gregory H. R. Henry[18], Janneke HilleRisLambers[19], Robert D. Hollister[20], Dirk N. Karger[21], Jens Kattge[9,22], Peter Manning[3], Janet S. Prevéy[23], Christian Rixen[23], Gabriela Schaepman-Strub[24], Haydn J. D. Thomas[1], Mark Vellend[25], Martin Wilmking[26], Sonja Wipf[23], Michele Carbognani[27], Luise Hermanutz[28], Esther Lévesque[29], Ulf Molau[30], Alessandro Petraglia[27], Nadejda A. Soudzilovskaia[31], Marko J. Spasojevic[32], Marcello Tomaselli[27], Tage Vowles[33], Juha M. Alatalo[34], Heather D. Alexander[35], Alba Anadon-Rosell[26,36,37], Sandra Angers-Blondin[1], Mariska te Beest[38,39], Logan Berner[16], Robert G. Björk[33,40], Agata Buchwal[41,42], Allan Buras[43], Katherine Christie[44], Elisabeth J. Cooper[45], Stefan Dullinger[46], Bo Elberling[47], Anu Eskelinen[9,48,49], Esther R. Frei[18,21], Oriol Grau[50,51], Paul Grogan[52], Martin Hallinger[53], Karen A. Harper[54], Monique M. P. D. Heijmans[55], James Hudson[56], Karl Hülber[46], Maitane Iturrate-Garcia[24], Colleen M. Iversen[57], Francesca Jaroszynska[23,58], Jill F. Johnstone[59], Rasmus Halfdan Jørgensen[60], Elina Kaarlejärvi[38,61], Rebecca Klady[62], Sara Kuleza[59], Aino Kulonen[23], Laurent J. Lamarque[29], Trevor Lantz[63], Chelsea J. Little[24,64], James D. M. Speed[65], Anders Michelsen[47,66], Ann Milbau[67], Jacob Nabe-Nielsen[68], Sigrid Schøler Nielsen[2], Josep M. Ninot[36,37], Steven F. Oberbauer[69], Johan Olofsson[38], Vladimir G. Onipchenko[70], Sabine B. Rumpf[46], Philipp Semenchuk[45,46], Rohan Shetti[26], Laura Siegwart Collier[28], Lorna E. Street[1], Katharine N. Suding[4], Ken D. Tape[71], Andrew Trant[28,72], Urs A. Treier[2,7,8], Jean-Pierre Tremblay[73], Maxime Tremblay[29], Susanna Venn[74], Stef Weijers[75], Tara Zamin[52], Noémie Boulanger-Lapointe[18], William A. Gould[76], David S. Hik[77], Annika Hofgaard[78], Ingibjörg S. Jónsdóttir[79,80], Janet Jorgenson[81], Julia Klein[82], Borgthor Magnusson[83], Craig Tweedie[84], Philip A. Wookey[85], Michael Bahn[86], Benjamin Blonder[87,88], Peter M. van Bodegom[89], Benjamin Bond-Lamberty[90], Giandiego Campetella[91], Bruno E. L. Cerabolini[92], F. Stuart Chapin III[93], William K. Cornwell[94], Joseph Craine[95], Matteo Dainese[96], Franciska T. de Vries[97], Sandra Díaz[98], Brian J. Enquist[99,100], Walton Green[101], Ruben Milla[102], Ülo Niinemets[103], Yusuke Onoda[104], Jenny C. Ordoñez[105], Wim A. Ozinga[106,107], Josep Penuelas[51,108], Hendrik Poorter[109,110], Peter Poschlod[111], Peter B. Reich[112,113], Brody Sandel[114], Brandon Schamp[115], Serge Sheremetev[116] & Evan Weiher[117]

[1]School of GeoSciences, University of Edinburgh, Edinburgh, UK. [2]Ecoinformatics and Biodiversity, Department of Bioscience, Aarhus University, Aarhus, Denmark. [3]Senckenberg Gesellschaft für Naturforschung, Biodiversity and Climate Research Centre (BiK-F), Frankfurt, Germany. [4]Department of Ecology and Evolutionary Biology, University of Colorado, Boulder, CO, USA. [5]National Ecological Observatory Network, Boulder, CO, USA. [6]Institute of Arctic and Alpine Research, University of Colorado, Boulder, CO, USA. [7]Arctic Research Center, Department of Bioscience, Aarhus University, Aarhus, Denmark. [8]Center for Biodiversity Dynamics in a Changing World (BIOCHANGE), Department of Bioscience, Aarhus University, Aarhus, Denmark. [9]German Centre for Integrative Biodiversity Research (iDiv) Halle-Jena-Leipzig, Leipzig, Germany. [10]Smithsonian Tropical Research Institute, Balboa, Panama. [11]European Commission, Joint Research Centre, Directorate D — Sustainable Resources, Bio-Economy Unit, Ispra, Italy. [12]Department of Physical Geography and Ecosystem Science, Lund University, Lund, Sweden. [13]Systems Ecology, Department of Ecological Science, Vrije Universiteit Amsterdam, Amsterdam, The Netherlands. [14]Arctic Centre, University of Lapland, Rovaniemi, Finland. [15]International Agency for Research in Cancer, Lyon, France. [16]School of Informatics, Computing and Cyber Systems, Northern Arizona University, Flagstaff, AZ, USA. [17]Bigelow Laboratory for Ocean Sciences, East Boothbay, ME, USA. [18]Department of Geography, University of British Columbia, Vancouver, British Columbia, Canada. [19]Biology Department, University of Washington, Seattle, WA, USA. [20]Biology Department, Grand Valley State University, Allendale, MI, USA. [21]Swiss Federal Research Institute WSL, Birmensdorf, Switzerland. [22]Max Planck Institute for Biogeochemistry, Jena, Germany. [23]WSL Institute for Snow and Avalanche Research SLF, Davos, Switzerland. [24]Department of Evolutionary Biology and Environmental Studies, University of Zurich, Zurich, Switzerland. [25]Département de biologie, Université de Sherbrooke, Sherbrooke, Québec, Canada. [26]Institute of Botany and Landscape Ecology, Greifswald University, Greifswald, Germany. [27]Department of Chemistry, Life Sciences and Environmental Sustainability, University of Parma, Parma, Italy. [28]Department of Biology, Memorial University, St. John's, Newfoundland and Labrador, Canada. [29]Département des Sciences de l'environnement et Centre d'études nordiques, Université du Québec à Trois-Rivières, Trois-Rivières, Québec, Canada. [30]Department of Biological and Environmental Sciences, University of Gothenburg, Gothenburg, Sweden. [31]Environmental Biology Department, Institute of Environmental Sciences, Leiden University, Leiden, The Netherlands. [32]Department of Evolution, Ecology and Organismal Biology, University of California Riverside, Riverside, CA, USA. [33]Department of Earth Sciences, University of Gothenburg, Gothenburg, Sweden. [34]Department of Biological and Environmental Sciences, Qatar University, Doha, Qatar. [35]Department of Forestry, Forest and Wildlife Research Center, Mississippi State University, Mississippi State, MS, USA. [36]Department of Evolutionary Biology, Ecology and Environmental Sciences, University of Barcelona, Barcelona, Spain. [37]Biodiversity Research Institute, University of Barcelona, Barcelona, Spain. [38]Department of Ecology and Environmental Science, Umeå University, Umeå, Sweden. [39]Environmental Sciences, Copernicus Institute of Sustainable Development, Utrecht University, Utrecht, The Netherlands. [40]Gothenburg Global Biodiversity Centre, Göteborg, Sweden. [41]Institute of Geoecology and Geoinformation, Adam Mickiewicz University, Poznan, Poland. [42]Department of Biological Sciences, University of Alaska, Anchorage, Anchorage, AK, USA. [43]Forest Ecology and Forest Management, Wageningen University and Research, Wageningen, The Netherlands. [44]The Alaska Department of Fish and Game, Anchorage, AK, USA. [45]Department of Arctic and Marine Biology, Faculty of Biosciences, Fisheries and Economics, UiT—The Arctic University of Norway, Tromsø, Norway. [46]Department of Botany and Biodiversity Research, University of Vienna, Vienna, Austria. [47]Center for Permafrost (CENPERM), Department of Geosciences and Natural Resource Management, University of Copenhagen, Copenhagen, Denmark. [48]Department of Physiological Diversity, Helmholtz Centre for Environmental Research—UFZ, Leipzig, Germany. [49]Department of Ecology and Genetics, University of Oulu, Oulu, Finland. [50]Global Ecology Unit, CREAF-CSIC-UAB, Cerdanyola del Vallès, Spain. [51]CREAF, Cerdanyola del Vallès, Spain. [52]Department of Biology, Queen's University, Kingston, Ontario, Canada. [53]Biology Department, Swedish Agricultural University (SLU), Uppsala, Sweden. [54]Biology Department, Saint Mary's University, Halifax, Nova Scotia, Canada. [55]Plant Ecology and Nature Conservation Group, Wageningen University and Research, Wageningen, The Netherlands. [56]British Columbia Public Service, Surrey, British Columbia, Canada. [57]Climate Change Science Institute and Environmental Sciences Division, Oak Ridge National Laboratory, Oak Ridge, TN, USA. [58]Institute of Biological and Environmental Sciences, University of Aberdeen, Aberdeen, UK. [59]Department of Biology, University of Saskatchewan, Saskatoon, Saskatchewan, Canada. [60]Forest and Landscape College, Department of Geosciences and Natural Resource Management, University of Copenhagen, Nødebo, Denmark. [61]Department of Biology, Vrije Universiteit Brussel (VUB), Brussels, Belgium. [62]Department of Forest Resources Management, Faculty of Forestry, University of British Columbia, Vancouver, British Columbia, Canada. [63]School of Environmental Studies, University of Victoria, Victoria, British Columbia, Canada. [64]Department of Aquatic Ecology, Eawag: Swiss Federal Institute of Aquatic Science and Technology, Dubendorf, Switzerland. [65]NTNU University Museum, Norwegian University of Science and Technology, Trondheim, Norway. [66]Department of Biology, University of Copenhagen, Copenhagen, Denmark. [67]Research Institute for Nature and Forest (INBO), Brussels, Belgium. [68]Department of Bioscience, Aarhus University, Roskilde, Denmark. [69]Department of Biological Sciences, Florida International University, Miami, FL, USA. [70]Department of Geobotany, Lomonosov Moscow State University, Moscow, Russia. [71]Institute of Northern Engineering, University of Alaska Fairbanks, Fairbanks, AK, USA. [72]School of Environment, Resources and Sustainability, University of Waterloo, Waterloo, Ontario, Canada. [73]Département de biologie, Centre d'études nordiques and Centre d'étude de la forêt, Université Laval, Quebec City, Québec, Canada. [74]Centre for Integrative Ecology, School of Life and Environmental Sciences, Deakin University, Burwood, Victoria, Australia. [75]Department of Geography, University of Bonn, Bonn, Germany. [76]USDA Forest Service International Institute of Tropical Forestry, Río Piedras, Puerto Rico. [77]Department of Biological Sciences, Simon Fraser University, Burnaby, British Columbia, Canada. [78]Norwegian Institute for Nature Research, Trondheim, Norway. [79]Faculty of Life and Environmental Sciences, University of Iceland, Reykjavík, Iceland. [80]University Centre in Svalbard, Longyearbyen, Norway. [81]Arctic National Wildlife Refuge, US Fish and Wildlife Service, Fairbanks, AK, USA. [82]Department of Ecosystem Science and Sustainability, Colorado State University, Fort Collins, CO, USA. [83]Icelandic Institute of Natural History, Gardabaer, Iceland. [84]University of Texas at El Paso, El Paso, TX, USA. [85]Biology and Environmental Sciences, Faculty of Natural Sciences, University of Stirling, Stirling, UK. [86]Institute of Ecology, University of Innsbruck, Innsbruck, Austria. [87]Environmental Change Institute, School of Geography and the Environment, University of Oxford, Oxford, UK. [88]Rocky Mountain Biological Laboratory, Crested Butte, CO, USA. [89]Institute of Environmental Sciences, Leiden University, Leiden, The Netherlands. [90]Joint Global Change Research Institute, Pacific Northwest National Laboratory, College Park, MD, USA. [91]School of Biosciences and Veterinary Medicine, Plant Diversity and Ecosystems Management Unit, University of Camerino, Camerino, Italy. [92]DiSTA, University of Insubria, Varese, Italy. [93]Institute of Arctic Biology, University of Alaska Fairbanks, Fairbanks, AK, USA. [94]School of Biological, Earth and Environmental Sciences, Ecology and Evolution Research Centre, UNSW Sydney, Sydney, New South Wales, Australia. [95]Jonah Ventures, Boulder, CO, USA. [96]Institute for Alpine Environment, Eurac Research, Bolzano, Italy. [97]School of Earth and Environmental Sciences, The University of Manchester, Manchester, UK. [98]Instituto Multidisciplinario de Biología Vegetal (IMBIV), CONICET and FCEFyN, Universidad Nacional de Córdoba, Córdoba, Argentina. [99]Department of Ecology and Evolutionary Biology, University of Arizona, Tucson, AZ, USA. [100]The Santa Fe Institute, Santa Fe, NM, USA. [101]Department of Organismic and Evolutionary Biology, Harvard University, Cambridge, MA, USA. [102]Área de Biodiversidad y Conservación. Departamento de Biología, Geología, Física y Química Inorgánica, Universidad Rey Juan Carlos, Madrid, Spain. [103]Estonian University of Life Sciences, Tartu, Estonia. [104]Graduate School of Agriculture, Kyoto University,

© 2018 Springer Nature Limited. All rights reserved.

Kyoto, Japan. [105]World Agroforestry Centre — Latin America, Lima, Peru. [106]Team Vegetation, Forest and Landscape Ecology, Wageningen Environmental Research (Alterra), Wageningen, The Netherlands. [107]Institute for Water and Wetland Research, Radboud University Nijmegen, Nijmegen, The Netherlands. [108]Global Ecology Unit CREAF-CSIC-UAB, Consejo Superior de Investigaciones Cientificas, Bellaterra, Spain. [109]Plant Sciences (IBG-2), Forschungszentrum Jülich GmbH, Jülich, Germany. [110]Department of Biological Sciences, Macquarie University, North Ryde, New South Wales, Australia. [111]Ecology and Conservation Biology, Institute of Plant Sciences, University of Regensburg, Regensburg, Germany. [112]Department of Forest Resources, University of Minnesota, St. Paul, MN, USA. [113]Hawkesbury Institute for the Environment, Western Sydney University, Penrith, New South Wales, Australia. [114]Department of Biology, Santa Clara University, Santa Clara, CA, USA. [115]Department of Biology, Algoma University, Sault Ste. Marie, Ontario, Canada. [116]Komarov Botanical Institute, St Petersburg, Russia. [117]Department of Biology, University of Wisconsin — Eau Claire, Eau Claire, WI, USA. *e-mail: anne.bjorkman@senckenberg.de

© 2018 Springer Nature Limited. All rights reserved.

METHODS

Below we describe the data, workflow (Extended Data Fig. 1b) and detailed methods used to conduct all analyses. No statistical methods were used to predetermine sample size.

Community composition data. Community composition data used for calculating CWM were compiled from a previous synthesis of tundra vegetation resurveys[2] (including many International Tundra Experiment (ITEX) sites) and expanded with additional sites (for example, Gavia Pass in the Italian Alps and three sites in Sweden) and years (for example, 2015 survey data added for Iceland sites, Qikiqtaruk–Herschel Island (QHI) and Alexandra Fiord; Supplementary Table 2). We included only sites for which community composition data were roughly equivalent to percentage cover (that is, excluding estimates approximating biomass), for a total of 117 sites (defined as plots in a single contiguous vegetation type) within 38 regions (defined as a CRU[41] grid cell). Plot-level surveys of species composition and cover were conducted at each of these sites between 1989 and 2015 (see the previous study[2] for more details regarding data collection and processing). On average, there were 15.2 plots per site. Repeat surveys were conducted over a minimum duration of 5 and up to 21 years between 1989 and 2015 (mean duration, 13.6 years), for a total of 1,781 unique plots and 5,507 plot–year combinations. Plots were either permanent (that is, staked; 62% of sites) or semi-permanent (38%), such that the approximate but not exact location was resurveyed. The vegetation monitoring sites were located in treeless Arctic or alpine tundra and ranged in latitude from 40° (Colorado Rockies) to 80° (Ellesmere Island, Canada) and were circumpolar in distribution (Fig. 1a and Supplementary Table 2). Our analyses only include vascular plants, because there was insufficient trait data for non-vascular species. Changes in bryophytes and other cryptogams are an important part of the trait and function change in tundra ecosystems[42,43], thus the incorporation of non-vascular plants and their traits is a future research priority.

Temperature extraction for community composition observations. We extracted summer (warmest quarter) and winter (coldest quarter) temperature estimates for each of the vegetation survey sites from both the WorldClim[44] (for long-term averages; http://www.worldclim.org/) and CRU[41] (for temporal trends; http://www.cru.uea.ac.uk/) gridded climate datasets. WorldClim temperatures were further corrected for elevation (based on the difference between the recorded elevation of a site and the mean elevation of the WorldClim grid cell) according to a correction factor of –0.005 °C per m increase in elevation. This correction factor was calculated by extracting the mean temperature and elevation (WorldClim 30-s resolution maps) of all cells that fall in a 2.5-km radius buffer around our sites and fitting a linear mixed model (with site as a random effect) to estimate the rate of temperature change with elevation.

The average long-term (1960–present) temperature trend across all sites was 0.26 °C (range, −0.06 to 0.49) and 0.43 °C (range, −0.15 to 1.32) per decade for summer and winter temperature, respectively.

Soil moisture for community composition observations. A categorical measure of soil moisture at each site was provided by the principle investigator of the site according to previously described methods[2,45]. Soil moisture was considered to be (1) dry when during the warmest month of the year the top 2 cm of the soil was dry to the touch; (2) mesic when soils were moist year round, but standing water was not present; and (3) wet when standing water was present during the warmest month of the year.

Soil moisture change for maps of environmental and trait change. We used high-resolution observations of soil moisture from the European Space Agency (ESA) CCI SM v.04.2 to estimate soil moisture change over time (Fig. 4c). To calculate the mean distribution of soil moisture, we averaged the observations for the period between 1979 and 2016. Because the ESA CCI SM temporal coverage is poor for our sites, temporal data were instead taken from the European Re-analysis (ERA-Interim; volumetric soil water layer 1) soil moisture estimates for the same time period. We downscaled the ERA-Interim data to the 0.05° resolution of ESA CCI SM v.04.2 using climatologically aided interpolation (delta change method)[46]. The change in soil water content was then calculated separately for each grid cell using linear regression with month as a predictor variable. To classify the soil moisture data into three categories (wet, mesic or dry) to match the community composition dataset, we used a quantile approach on the mean soil moisture within the extent of the Arctic. We assigned the lowest quantile to dry and the highest to wet conditions. For the trends in soil moisture between 1979 and 2016, we first calculated the percentage change in relation to the mean, and then calculated the change based on the categorical data (for example, 5% change from category 1 (dry) to category 2 (mesic)).

Changes in water availability for analysis. Although the strong effect of soil moisture on spatial temperature–trait relationships suggests that change in water availability over time will play an important part in mediating trait change, we did not use the CRU estimates of precipitation change over time, because of issues with precipitation records at high latitudes and the inability of gridded datasets to capture localized precipitation patterns[47,48]. The CRU precipitation trends at our sites included many data gaps filled by long-term mean values, especially at high-latitude sites[45]. As a purely exploratory analysis, we used the downscaled ERA-Interim data described above to investigate whether trait change is related to summer soil moisture change (June, July and August; Extended Data Fig. 5b). However, we caution that changes in soil moisture in our tundra sites are primarily controlled by the timing of the snow melting, soil drainage, the permafrost table and local hydrology[25], and as such precipitation records and coarse-grain remotely sensed soil-moisture change data are unlikely to accurately represent local changes in soil water availability. For this reason, we did not use the ERA-Interim data to explore spatial relationships between temperature, moisture and community traits, as the categorical soil moisture data (described above) were collected specifically within each community composition site and are therefore a more accurate representation of long-term mean soil moisture conditions in that specific location.

Trait data. Continuous trait data (adult plant height, leaf area (average one-sided area of a single leaf), SLA (leaf area per unit of leaf dry mass), leaf nitrogen content (per unit of leaf dry mass), and LDMC (leaf dry mass per unit of leaf fresh mass) (Fig. 1a, Extended Data Fig. 1a and Supplementary Table 1) were extracted from the TRY[49] 3.0 database (https://www.try-db.org/TryWeb/Home.php). We also ran a field and data campaign in 2014–2015 to collect additional in situ tundra trait data (the 'Tundra Trait Team' (TTT) dataset[50]) to supplement existing TRY records. All species names from the vegetation monitoring sites, TRY and TTT were matched to accepted names in The Plant List using the R package Taxonstand[51] (v.1.8) before merging the datasets. Community-level traits (woodiness and evergreenness) were derived from functional group classifications for each species[2]. Woodiness is estimated as the proportion (abundance) of woody species in the plot, whereas evergreenness is the proportion of evergreen woody species abundance out of all woody species (evergreen plus deciduous) in a plot. Because some sites did not contain any woody species (and thus the proportion of evergreen woody species could not be calculated), this trait is only estimated for 98 of the 117 total sites.

Data cleaning for TRY data. TRY trait data were subjected to a multi-step cleaning process. First, all values that did not represent individual measurements or approximate species means were excluded. When a dataset within TRY contained only coarse plant height estimates (for example, estimated to the nearest foot), we removed these values unless no other estimate of height for that species was available. We then identified overlapping datasets within TRY and removed duplicate observations whenever possible. The following datasets were identified as having partially overlapping observations: GLOPNET (Global Plant Trait Network Database), The LEDA Traitbase, Abisko and Sheffield Database, Tundra Plant Traits Database and Kew Seed Information Database (SID).

We then removed duplicates within each TRY dataset (for example, if a value is listed once as 'mean' and again as 'best estimate') by first calculating the ratio of duplicated values within each dataset, and then removing duplicates from datasets with more than 30% duplicated values. This cut-off was determined by manual evaluation of datasets at a range of thresholds. Datasets with fewer than 30% duplicated values were not removed in this way as any internally duplicate values were assumed to be true duplicates (that is, two different individuals were measured and happened to have the same measurement value).

We also removed all species mean observations from the 'Niwot Alpine Plant Traits' database and replaced it with the original individual observations provided by M.J.S.

Data cleaning for the combined TRY and TTT dataset. Both datasets were checked for improbable values, with the goal of excluding likely errors or measurements with incorrect units but without excluding true extreme values. We followed a series of data-cleaning steps, in each case identifying whether a given observation (x) was likely to be erroneous (that is, 'error risk') by calculating the difference between x and the mean (excluding x) of the taxon and then dividing by the standard deviation of the taxon.

We used a hierarchical data-cleaning method, because the standard deviation of a trait value is related to the mean and sample size. First, we checked individual records against the entire distribution of observations of that trait and removed any records with an error risk greater than 8 (that is, a value more than 8 standard deviations away from the trait mean). For species that occurred in four or more unique datasets within TRY or TTT (that is, different data contributors), we estimated a species mean per dataset and removed observations for which the species mean error risk was greater than 3 (that is, the species mean of that dataset was more than 3 standard deviations away from the species mean across all datasets). For species that occurred in fewer than four unique datasets, we estimated a genus mean per dataset and removed observations in datasets for which the error risk based on the genus mean was greater than 3.5. Finally, we compared individual records directly to the distribution of values for that species. For species with more than four records, we excluded values above an error risk Y, where Y was dependent on the number of records of that species and ranged from an error risk of 2.25 for species with fewer than 10 records to an error risk of 4 for species with more than 30 records. For species with four or fewer records, we manually checked trait

© 2018 Springer Nature Limited. All rights reserved.

values and excluded only those that were obviously erroneous, based on our expert knowledge of these species.

This procedure was performed on the complete tundra trait database, including species and traits not presented here. In total 2,056 observations (1.6%) were removed. In all cases, we visually checked the excluded values against the distribution of all observations for each species to ensure that our trait cleaning protocol was reasonable.

Trait data were distributed across latitudes within the tundra biome (Extended Data Fig. 1a). All trait observations with latitude and longitude information were mapped and checked for implausible values (for example, falling in the ocean). These values were corrected from the original publications or by contacting the data contributor whenever possible.

Final trait database. After removing duplicates and outliers as described above, we retained 56,048 unique trait observations (of which 18,613 are contained in TRY and 37,435 were newly contributed by the TTT[50] field campaign) across the five continuous traits of interest. Of the 447 identified species in the ITEX dataset, 386 (86%) had trait data available from TRY or TTT for at least one trait (range 52–100% per site). Those species without trait data generally represent rare or uncommon species unique to each site; on average, trait data were available for 97% of total plant cover across all sites (range 39–100% per site; Supplementary Table 1).

Temperature extraction for trait observations. WorldClim climate variables were extracted for all trait observations with latitude and longitude values recorded (53,123 records in total, of which 12,380 were from TRY and 33,621 from TTT). Because most observations did not include information about elevation, temperature estimates for individual trait observations were not corrected for elevation and thus represent the temperature at the mean elevation of the WorldClim grid cell.

Analyses. *Terminology.* Here we provide a brief description of acronyms and symbols used in the methods and model equations. α is used to designate lower-level model intercepts; β is used to designate lower-level model slopes; γ is used to designate the model parameters of interest (for example, the temperature–trait relationship); CWM designates the mean trait value of all species in a plot, weighted by their abundance in the plot; CWM + ITV designates CWM adjusted with the estimated contribution of ITV based on the intraspecific temperature–trait relationship of each species; and ITV designates variation in trait values within the same species (that is, intraspecific trait variation).

Models. All analyses were conducted in JAGS and/or Stan through R (v.3.3.3) using packages rjags[52] (v.4.6) and rstan[53] (v.2.14.1). In all cases, models were run until convergence was reached, which was assessed both visually in traceplots and by ensuring that all Gelman–Rubin convergence diagnostic ($\hat{R}$)[54] values were less than 1.1.

A major limitation of the species mean trait approach, which is often used in analyses of environment–trait relationships, has been the failure to account for ITV, which could be as or more important than interspecific variation[55,56]. We addressed this issue by using a hierarchical analysis that incorporates both within-species and community-level trait variation across climate gradients to estimate trait change over space and time at the biome scale. We used a Bayesian approach that accounts for the hierarchical spatial (plots within sites within regions) and taxonomic (intra- and inter-specific variation) structure of the data as well as uncertainty in estimated parameters introduced through absences in trait records for some species, or through taxa that were identified to genus or functional group (rather than species) in vegetation surveys.

ITV. To calculate intraspecific temperature–trait relationships, we used a subset of the trait dataset containing only those species for which traits had been measured in at least four unique locations spanning a temperature range of at least 10% of the entire temperature range (2.6 °C and 5.0 °C for summer and winter temperature, respectively), and for which the latitude and longitude of the measured individual or group of individuals was recorded. The number of species meeting these criteria varied by trait and temperature variable: 108 and 109 for SLA, 80 and 86 for plant height, 74 and 72 for leaf nitrogen, 85 and 76 for leaf area, and 43 and 52 for LDMC, for summer and winter temperature, respectively. These species counts correspond to 53–73% of the abundance in the community. The relationship between each trait and temperature (Fig. 2b) was estimated from a Bayesian hierarchical model, with temperature as the predictor variable and species (sp) and dataset-by-location (d) modelled as random effects:

$$\text{trait}_i^{\text{observed}} \sim \log\text{normal}(\alpha_{\text{sp},d}, \sigma_{\text{sp}})$$

$$\alpha_{\text{sp},d} \sim \text{Normal}(\alpha_{\text{sp}} + \beta_{\text{sp}} T_d, \sigma_1)$$

$$\beta_{\text{sp}} \sim \text{Normal}(B, \sigma_2)$$

$$\alpha_{\text{sp}} \sim \text{Normal}(A, \sigma_3)$$

in which the tilde ($\sim$) indicates 'distributed as', T indicates temperature, i represents each trait observation and A and B are the intercept and slope hyperparameters, respectively. Because LDMC represents a ratio and is thus bound between 0 and 1, we used a beta error distribution for this trait. Temperature values were mean-centred within each species. We used non-informative priors for all coefficients.

We further explored whether the strength of intraspecific temperature–height relationships varied by functional group. We find that all functional groups (including dwarf shrubs, which are genetically limited in their ability to grow upright) show similar temperature–trait relationships (Extended Data Fig. 9a). These results suggest that intraspecific temperature–height relationships are not just a consequence of individual growth differences, and are not restricted to particular functional groups with greater capacity for vertical growth (for example, tall shrubs and graminoids versus dwarf shrubs and certain forb species).

Calculation of CWM values. We calculated the CWM (that is, the mean trait value of all species in a plot, weighted by the abundance of each species), for all plots within a site. We used a Bayesian approach to calculate trait means for every species (s) using an intercept-only model (such that the intercept per species (α_s) is equivalent to the mean trait value of the species) and variation per species (σ_s) with a lognormal error distribution:

$$\text{trait}_i^{\text{observed}} \sim \log\text{normal}(\alpha_s, \sigma_s)$$

Because LDMC represents a ratio and is thus bound between 0 and 1, we used a beta error distribution instead of log normal for this trait. When a species was measured multiple times in several different locations, we additionally included a random effect of dataset-by-location (d) to reduce the influence of a single dataset with many observations at one site when calculating the mean per species:

$$\text{trait}_i^{\text{observed}} \sim \log\text{normal}(\alpha_{s,d}, \sigma_d)$$

$$\alpha_{s,d} \sim \text{Normal}(\alpha_s, \sigma_s)$$

We used non-informative priors for all species intercept parameters for which there were four or more unique trait observations, so that the species-level intercept and variance around the intercept per species were estimated from the data. To avoid removing species with little or no trait data from the analyses, we additionally used a 'gap-filling' approach that enabled us to estimate the trait mean of each species while accounting for uncertainty in the estimation of this mean. For species with fewer than four but more than one trait observation, we used a normal prior with the mean equal to the mean of the observation(s) and variance estimated based on the mean mean:variance ratio across all species. In other words, we calculated the ratio of mean trait values to the standard deviation of those trait values per species for all species with greater than four observations, then took the mean of these ratios across all species and multiplied this number by the mean of species X (in which X is a species with 1–4 observations) to get the prior for σ. For species with no observations (see Supplementary Table 1), we used a prior mean equal to the mean of all species in the same genus and a prior variance estimated based on the mean mean:variance ratio of all species in that genus or 1.5× the mean, whichever was lower. If there were no other species in the same genus, then we used a prior mean equal to the mean of all other species in the family and a prior variance estimated based on the mean mean:variance ratio of all species in the family or 1.5× the mean, whichever was lower.

Incorporating uncertainty in species traits to calculate CWM values. To include uncertainty about species trait means (owing to ITV, missing trait information for some species or when taxa were identified to genus or functional group rather than species) in subsequent analyses, we estimated community-level trait values per plot by sampling from the posterior distribution (mean ± s.d.) of each species intercept estimate and multiplying this distribution by the relative abundance of each species in the plot to get a CWM distribution per plot (p) per year (y):

$$\text{Normal}\left(\text{CWM}_{p,y}^{\text{mean}}, \text{CWM}_{p,y}^{\text{s.d.}}\right)$$

This approach generates a distribution of CWM values per plot that propagates the uncertainty in the mean estimate of each trait for each species into the plot-level (CWM) estimate. By using a Bayesian approach, we are able to carry through uncertainty in mean estimates of traits to all subsequent analyses and reduce the potential for biased or deceptively precise estimates due to missing trait observations.

Partitioning turnover and estimating contribution of ITV to temperature–trait relationships. To assess the degree to which the spatial temperature–trait relationships are caused by species turnover versus shifts in abundance among sites, we repeated each analysis using the non-weighted community mean (all species weighted equally) of each plot. Temperature–trait relationships estimated with non-weighted community means are due only to species turnover across sites.

© 2018 Springer Nature Limited. All rights reserved.

Finally, we assessed the potential contribution of ITV to the community-level temperature–trait relationship by using the modelled intraspecific temperature–trait relationship (see 'ITV') to predict trait 'anomaly' values for each species at each site based on the temperature of that site in a given year relative to its long-term average. An intraspecific temperature–trait relationship could not be estimated for every species owing to an insufficient number of observations for some species. Therefore, we used the mean intraspecific temperature–trait slope across all species to predict trait anomalies for species without intraspecific temperature–trait relationships.

Site- and year-specific species trait estimates were then used to calculate ITV-adjusted CWM (CWM + ITV) for each plot in each measured year, and modelled as for CWM alone. As these adjusted values are estimated relative to the mean value of each species, the spatial temperature–trait relationship that includes this adjustment does not remove any bias in the underlying species mean data. For example, if southern tundra species tend to be measured at the southern edge of their range while northern tundra species tend to be measured at the northern edge of their range, the overall spatial temperature–trait relationship could appear stronger than it really is for species with temperature-related intraspecific variation. This is a limitation of any species-mean approach.

Estimates of temporal CWM + ITV temperature–trait relationships are not prone to this same limitation as they represent relative change, but should also be interpreted with caution as intraspecific temperature–trait relationships may be due to genetic differences among populations rather than plasticity, thus suggesting that trait change would not occur immediately with warming. We therefore caution that the CWM + ITV analyses represent estimates of the potential contribution of ITV to overall CWM temperature–trait relationships over space and time, but should not be interpreted as measured responses.

In summary, we incorporate intraspecific variation into our analyses in three ways. First, by using the posterior distribution (rather than a single mean value) of species trait mean estimates in our calculations of CWM values per plot, so that information about the amount of variation within species is incorporated into all the analyses in our study. Second, by explicitly estimating intraspecific temperature–trait relationships based on the spatial variation in traits among individuals of the same species. Third, by using these modelled temperature–trait relationships to inform estimates of the potential contribution of ITV to overall (CWM + ITV) temperature–trait relationships over space and time.

Spatial community trait models. To investigate spatial relationships in plant traits with summer or winter temperature and soil moisture (Fig. 2a, c), we used a Bayesian hierarchical modelling approach in which soil moisture and soil moisture × temperature vary at the site level while temperature varies by WorldClim region (unique WorldClim grid × elevation groups). In total, there were 117 sites (s) nested within 73 WorldClim regions (r). We used only the first year of survey data at each site to estimate spatial relationships in community traits.

$$\mathrm{CWM}_p^{\mathrm{mean}} \sim \mathrm{Normal}\left(\alpha_s + \alpha_r, \mathrm{CWM}_p^{\mathrm{s.d.}}\right)$$

$$\alpha_s \sim \mathrm{Normal}\left(\gamma_1 M_s + \gamma_2 M_s T_s, \sigma_1\right)$$

$$\alpha_r \sim \mathrm{Normal}\left(\gamma_0 + \gamma_3 T_r, \sigma_2\right)$$

in which M indicates moisture, $\mathrm{CWM}_p^{\mathrm{mean}}$ is the mean of the posterior distribution of the CWM estimate per plot (p) and $\mathrm{CWM}_p^{\mathrm{s.d.}}$ is the standard deviation of the posterior distribution of the CWM estimate per plot (see 'Incorporating uncertainty in species traits to calculate CWM values'). See Supplementary Information for complete STAN code.

As woodiness and evergreenness represent proportional data (bound between 0 and 1, inclusive), we used a beta–Bernoulli mixture model of the same structure as above to estimate trait–temperature–moisture relationships for these traits (Extended Data Fig. 3a, b). The discrete and continuous components of the data were modelled separately, with mixing occurring at the site- and region-level estimates (α_s and α_r).

Because Arctic and alpine tundra sites might differ in their trait–environment relationships owing to environmental differences (for example, in soil drainage), we also performed a version of the spatial community trait analyses in which the elevation of each site is visually indicated (not modelled; Extended Data Fig. 9b). We did not attempt to separately analyse trait–environment relationships for Arctic and alpine sites owing to the ambiguity in defining this cut-off (that is, many sites can be categorized as both Arctic and alpine, particularly in Scandinavia and Iceland) and because of the small number of southern, high-alpine sites (European Alps and Colorado Rockies).

For estimation of the overall temperature–trait relationship, we used a model structure similar to that above but with only temperature as a predictor (that is, without soil moisture). This model was used for both CWM and non-weighted mean estimates to determine the degree to which temperature–trait relationships over space are due to species turnover alone (non-weighted mean) and for CWM + ITV plot-level estimates to determine the likely additional contribution of ITV to the overall temperature–trait relationship, as described above.

Standardized effect sizes for CWM temperature–trait relationships (Fig. 2c) were obtained by dividing the slope of the temperature–trait relationship by the standard deviation of the CWM model residuals. Effect sizes for ITV, turnover only and CWM + ITV were estimated relative to the CWM value for that same trait based on the slope values of each temperature-trait relationship.

Trait change over time. Change over time (Fig. 3a, b) was modelled at the CRU grid cell (region) level. We first estimated a region-by-year (r, y) effect to account for the non-independence of observations made within the same region and year. We also included site (s) as a random effect when there was more than one site per region (to account for non-independence of sites within a region) and plot (p) as a random effect for those sites with permanent (repeating) plots (to account for repeated measures on the same plot over time):

$$\mathrm{CWM}_{p,y}^{\mathrm{mean}} \sim \mathrm{Normal}\left(\alpha_p + \alpha_s + \alpha_{r,y}, \mathrm{CWM}_{p,y}^{\mathrm{s.d.}}\right)$$

in which $\mathrm{CWM}_{p,y}^{\mathrm{mean}}$ is the mean of the posterior distribution of the CWM estimate per plot (p) in a given year (y) and $\mathrm{CWM}_{p,y}^{\mathrm{s.d.}}$ is the standard deviation of the posterior distribution of the CWM estimate per plot and year (see 'Incorporating uncertainty in species traits to calculate CWM values'). For non-permanent plots and for sites that were the only site within a region, α_p or α_s, respectively, were set to 0.

Region-level slopes were then used to fit an average trend of community trait values over time, in which Y represents calendar year (centred within each region) as a linear predictor:

$$\alpha_{r,y} \sim \mathrm{Normal}\left(\alpha_r + \beta_r Y_{r,y}, \sigma_0\right)$$

$$\beta_r \sim \mathrm{Normal}\left(B, \sigma_1\right)$$

$$\alpha_r \sim \mathrm{Normal}\left(A, \sigma_2\right)$$

in which A and B are the intercept and slope hyperparameters, respectively. See Supplementary Information for complete STAN code. This model was used for both CWM and non-weighted mean plot-level estimates to determine the degree to which temporal trait change is due to species turnover alone (non-weighted mean) and for CWM + ITV plot-level estimates to determine the potential additional contribution of ITV to overall trait change. We did not account for temporal autocorrelation in these models as most plots were not measured annually (average survey interval = 7.2 years) and did not have more than three observations over the study period (average number of survey years per plot = 3.1).

Standardized effect sizes for CWM change over time (Fig. 3b) were obtained by dividing the slope of overall trait change over time (mean hyperparameter across 117 sites) by the standard deviation of the slope estimates per site. Effect sizes for turnover-only and CWM + ITV changes are estimated relative to the CWM change value for that trait based on the slope values of each.

To estimate the change in the proportion of woody and evergreen species over time (CWM change only; Extended Data Fig. 3c, d) we used a beta–Bernoulli mixture model of the same form described above. The discrete and continuous components of the data were modelled separately, with mixing occurring at the region × year effect ($\alpha_{r,y}$). We additionally assessed whether the rate of observed trait change over time was related to the duration of vegetation monitoring at each site. There was no influence of monitoring duration for any trait (data not shown).

Temperature sensitivity. Temperature sensitivity (Fig. 3c) was modelled as the variation in CWM trait values with variation in the five-year mean temperature (that is, the mean temperature of the survey year and the four preceding years). A four-year lag was chosen because this interval has been shown to best explain vegetation change in tundra[20] and alpine[29] plant communities. The model specifics are exactly as shown above (see 'Trait change over time'), but with temperature in the place of the linear year predictor (Y). Temperatures were centred within each region.

Observed versus expected changes in traits. To compare rates of observed versus expected community trait change (Fig. 4a), we first calculated the mean rate of temperature change across the 38 regions in our study, and then estimated the expected degree of change in each trait over the same period based on this temperature change and the spatial relationship between temperature and CWM trait values (see 'Spatial community trait models'). We then compared this expected trait change to actual trait change over time (see 'Trait change over time'). To create Fig. 4a, we used the overall predicted mean value of each trait in the first year of survey (1989) as an intercept, and then used the expected and observed rates of trait change (± uncertainty) to predict community trait values in each year

© 2018 Springer Nature Limited. All rights reserved.

thereafter. We subtracted the intercept from all predicted values to show trait change as an anomaly (difference from 0). The difference between the expected (black) and observed (coloured) lines in Fig. 4a represents a deviation from expected. To calculate total trait change, including the estimated contribution of intraspecific change (coloured dashed lines), we followed the same procedure as described for 'observed' trait change but where this observed change was based on plot-level CWM + ITV estimates that varied by year based on the temperature in that year and the temperature–trait relationship per species (see 'Partitioning turnover and estimating contribution of ITV to temperature–trait relationships').

Trait change versus changes in temperature and soil moisture. To determine whether the rate of trait change can be explained by the rate of temperature change at a site, the (static) level of soil moisture of a site or their interaction (Extended Data Fig. 5), we modelled the rate of trait change (see 'Trait change over time') and compared it to the rate of temperature change over the same time interval (with a lag of four years) and soil moisture:

$$\beta_r \sim \text{Normal}(\gamma_0 + \gamma_1 T_r + \gamma_2 M_r + \gamma_3 T_r M_r, \sigma)$$

in which β_r is the rate of trait change per region (Extended Data Fig. 5a). When sites within a region were measured over different intervals or contained different soil moisture estimates, they were modelled separately to match with temperature change estimates over the same interval and soil moisture estimates, which varied at the site level.

We also conducted this analysis using estimates of soil moisture change (with a lag of four years) from downscaled ERA-Interim data (volumetric soil water layer 1). This model took the same form as above, but with moisture change in place of static soil moisture estimates (Extended Data Fig. 5b). Trait change was modelled at the site (rather than region) level, because estimates of soil moisture change varied at the site level. Because ERA-Interim data were not available for every site, this analysis was conducted with a total of 101 rather than 117 sites. We note that the results of this analysis should be interpreted with caution, as local changes in soil moisture may not be well-represented by coarse-scale remotely sensed data, as previously described.

Species gains and losses as a function of traits. We explored whether turnover in community composition was related to species' traits (Extended Data Fig. 6). We estimated species gains and losses at the site (rather than plot) level to reduce the effect of random fluctuations in species presences and absences due to observer error or sampling methodology. Thus, sites with repeating and non-repeating plots were treated the same. A 'gain' was defined as a species that did not occur in a site in the first survey year but did in the last survey year, whereas a 'loss' was the reverse. We then modelled the probability of gain or loss separately as a function of the mean trait value of each species. For example, for gains, all newly observed species received a response type of 1 whereas all other species in the site received a response type of 0:

$$\text{response}_i \sim \text{Bernoulli}(\alpha_s + \alpha_r + \beta_r \text{trait}_i)$$

$$\alpha_r \sim \text{Normal}(A, \sigma_1)$$

$$\beta_r \sim \text{Normal}(B, \sigma_2)$$

$$\alpha_s \sim \text{Normal}(0, \sigma_r)$$

We included a random effect for site (s) only when there were multiple sites within the same region (r), otherwise α_s was set to 0. We considered the responses of species to be related to a given trait when the 95% credible interval on the slope hyperparameter (B) did not overlap zero.

Trait projections with warming. We projected trait change for the minimum (Representative Concentration Pathways (RCP)2.6) and maximum (RCP8.5) IPCC carbon emission scenarios from the NIMR HadGEM2-AO Global Circulation Model (Extended Data Fig. 7). We used the midpoint years of the WorldClim (1975) and HadGem2 (2090) estimates to calculate the expected rate of temperature change over this time period. We then predicted trait values for each year into the future based on the projected rate of temperature change and the spatial relationship between temperature and community trait values (see 'Spatial community trait models').

These projections are not intended to predict actual expected changes in traits over the next century, as many other factors not accounted for here will also influence this change. In particular, future changes in functional traits will probably depend on concurrent changes in moisture availability, which are less well understood than temperature change. Recent modelling efforts predict increases in precipitation across much of the Arctic[57], but it is unknown whether increasing precipitation will also lead to an increase in soil moisture and/or water availability for plants, as the drying effect of warmer temperatures (for example, due to increased evaporation and/or decreased duration of snow cover[58]) may outweigh the effect of increased precipitation. Instead, these projections are an attempt to explore theoretical changes in traits over a long-term period when using a space-for-time substitution approach.

Principal component analysis. We performed an ordination of CWM values per plot on all seven traits (Extended Data Fig. 8). Because community evergreenness could only be estimated for plots with at least one woody species, the total number of plots included in this analysis is reduced compared to the entire dataset (1,098 plots out of 1,520 in total). We used the R package vegan[59] (v.2.4.6) to conduct a principal component analysis (PCA) of these data. This analysis uses only trait means per plot, and therefore information about CWM uncertainty due to ITV and/or missing species is lost. The analysis was performed on log-transformed trait values[49]. We extracted the axis coordinates of each plot from the PCA and used the spatial trait–temperature–moisture model described above (see 'Spatial community trait models') to determine whether plot positions along both PCA axes varied with temperature, moisture and their interaction.

Trends in the abundance of species. To provide more insights into the species-specific changes that have occurred over time in tundra ecosystems, we calculated trends in abundance for the most common (widespread and abundant) species in the community composition dataset (Supplementary Table 10). We estimated trends for all species that occurred in at least five sites at a minimum abundance of 5% cover (mean of all plots within a site) across all years. We additionally included species that occurred at low abundance (1% or more) but were widespread (at least 10 sites). This technique yielded a total of 79 species. Abundance changes were modelled as described for trait change over time, but because abundance (proportion of plot cover) is bounded between 0 and 1, inclusive, we used a beta–Bernoulli mixture model. Abundance change was then estimated per species (sp) across all regions (r):

$$\alpha_{\text{sp},r,y} \sim \text{Normal}(\alpha_{\text{sp},r} + \beta_{\text{sp},r} Y_{\text{sp},r,y}, \sigma_{\text{sp}})$$

$$\beta_{\text{sp},r} \sim \text{Normal}(\text{B}_{\text{sp}}, \sigma_1)$$

$$\alpha_{sp,r} \sim \text{Normal}(\text{A}_{\text{sp}}, \sigma_2)$$

We additionally extracted region-specific slopes per species ($\beta_{\text{sp},r}$) to calculate a proportion of regions in which a given species was increasing or decreasing ('Prop. Increase' and 'Prop. Decrease' in Supplementary Table 10). Because regional slopes are modelled as random effects, these estimates are not entirely independent (that is, they will be pulled towards the overall species mean slope), but provide an approximate estimate of whether directional trends in abundance are consistent across the range of a species.

Reporting summary. Further information on research design is available in the Nature Research Reporting Summary linked to this paper.

Code availability. STAN code for the two main models (spatial temperature–moisture–trait relationships and community trait change over time) is provided in the Supplementary Information. Code for trait data cleaning is provided in the Tundra Trait Team data repository[50] (https://github.com/ShrubHub/TraitHub, https://tundratraitteam.github.io/).

Data availability

Trait data. Data compiled through the Tundra Trait Team are publicly accessible[50]. The public TTT database includes traits not considered in this study as well as tundra species that do not occur in our vegetation survey plots, for a total of nearly 92,000 trait observations on 978 species. Additional trait data from the TRY trait database can be requested at https://www.try-db.org/.

Composition data. Most sites and years of the vegetation survey data included in this study are available in the Polar Data Catalogue (ID 10786_iso). Much of the individual site-level data has additionally been made available in the BioTIME database[60] (https://synergy.st-andrews.ac.uk/biotime/biotime-database/).

41. Harris, I., Jones, P. D., Osborn, T. J. & Lister, D. H. Updated high-resolution grids of monthly climatic observations – the CRU TS3.10 Dataset. *Int. J. Climatol.* **34**, 623–642 (2014).
42. Blok, D. et al. The cooling capacity of mosses: controls on water and energy fluxes in a Siberian tundra site. *Ecosystems* **14**, 1055–1065 (2011).
43. Soudzilovskaia, N. A., van Bodegom, P. M. & Cornelissen, J. H. C. Dominant bryophyte control over high-latitude soil temperature fluctuations predicted by heat transfer traits, field moisture regime and laws of thermal insulation. *Funct. Ecol.* **27**, 1442–1454 (2013).
44. Hijmans, R. J., Cameron, S. E., Parra, J. L., Jones, J. L. & Jarvis, A. Very high resolution interpolated climate surfaces for global land areas. *Int. J. Climatol.* **25**, 1965–1978 (2005).
45. Myers-Smith, I. H. et al. Climate sensitivity of shrub growth across the tundra biome. *Nat. Clim. Change* **5**, 887–891 (2015).

© 2018 Springer Nature Limited. All rights reserved.

46. Willmott, C. J. & Robeson, S. M. Climatologically aided interpolation (CAI) of terrestrial air temperature. *Int. J. Climatol.* **15**, 221–229 (1995).
47. Sperna Weiland, F. C., Vrugt, J. A., van Beek, R. (L.) P. H., Weerts, A. H. & Bierkens, M. F. P. Significant uncertainty in global scale hydrological modeling from precipitation data errors. *J. Hydrol.* **529**, 1095–1115 (2015).
48. Beguería, S., Vicente Serrano, S. M., Tomás Burguera, M. & Maneta, M. Bias in the variance of gridded data sets leads to misleading conclusions about changes in climate variability. *Int. J. Climatol.* **36**, 3413–3422 (2016).
49. Kattge, J. et al. TRY—a global database of plant traits. *Glob. Change Biol.* **17**, 2905–2935 (2011).
50. Bjorkman, A. D. et al. Tundra Trait Team: a database of plant traits spanning the tundra biome. *Glob. Ecol. Biogeogr.* https://doi.org/10.1111/geb.12821 (2018).
51. Cayuela, L., Granzow-de la Cerda, Í., Albuquerque, F. S. & Golicher, D. J. taxonstand: an R package for species names standardisation in vegetation databases. Methods *Ecol. Evol.* **3**, 1078–1083 (2012).
52. Plummer, M. rjags: Bayesian graphical models using MCMC. R package version 4.6 https://CRAN.R-project.org/package=rjags (2016).
53. Stan Development Team. RStan: the R interface to Stan. R package version 2.14.1 http://mc-stan.org/ (2016).
54. Gelman, A. & Rubin, D. B. Inference from iterative simulation using multiple sequences. *Stat. Sci.* **7**, 457–472 (1992).
55. Messier, J., McGill, B. J. & Lechowicz, M. J. How do traits vary across ecological scales? A case for trait-based ecology. *Ecol. Lett.* **13**, 838–848 (2010).
56. Violle, C. et al. The return of the variance: intraspecific variability in community ecology. *Trends Ecol. Evol.* **27**, 244–252 (2012).
57. Bintanja, R. & Selten, F. M. Future increases in Arctic precipitation linked to local evaporation and sea-ice retreat. *Nature* **509**, 479–482 (2014).
58. AMAP. *Snow, Water, Ice and Permafrost in the Arctic (SWIPA) 2017*. https://www.amap.no (Arctic Monitoring and Assessment Programme, 2017).
59. Oksanen, J., Blanchet, F., Kindt, R. & Legendre, P. vegan: Community Ecology Package. R package version 2.4.6 https://CRAN.R-project.org/package=vegan (2011).
60. Dornelas, M. et al. BioTIME: A database of biodiversity time series for the Anthropocene. *Glob. Ecol. Biogeogr.* **27**, 760–786 (2018).
61. Chapin, F. S. III, BretHarte, M. S., Hobbie, S. E. & Zhong, H. L. Plant functional types as predictors of transient responses of arctic vegetation to global change. *J. Veg. Sci.* **7**, 347–358 (1996).
62. Weiher, E. et al. Challenging Theophrastus: a common core list of plant traits for functional ecology. *J. Veg. Sci.* **10**, 609–620 (1999).
63. Violle, C. et al. Let the concept of trait be functional! *Oikos* **116**, 882–892 (2007).
64. Hudson, J. M. G. & Henry, G. H. R. Increased plant biomass in a high Arctic heath community from 1981 to 2008. *Ecology* **90**, 2657–2663 (2009).
65. De Deyn, G. B., Cornelissen, J. H. C. & Bardgett, R. D. Plant functional traits and soil carbon sequestration in contrasting biomes. *Ecol. Lett.* **11**, 516–531 (2008).
66. Kunstler, G. et al. Plant functional traits have globally consistent effects on competition. *Nature* **529**, 204–207 (2016).
67. Gaudet, C. L. & Keddy, P. A. A comparative approach to predicting competitive ability from plant traits. *Nature* **334**, 242–243 (1988).
68. Westoby, M., Falster, D. S., Moldes, A. T., Vesk, P. A. & Wright, I. J. Plant ecological strategies: some leading dimensions of variation between species. *Annu. Rev. Ecol. Syst.* **33**, 125–159 (2002).
69. Moles, A. T. & Leishman, M. R. *Seedling Ecology and Evolution* (Cambridge Univ. Press, Cambridge, 2008).
70. Sturm, M. et al. Snow–shrub interactions in Arctic tundra: a hypothesis with climatic implications. *J. Clim.* **14**, 336–344 (2001).
71. Loranty, M. M., Berner, L. T., Goetz, S. J., Jin, Y. & Randerson, J. T. Vegetation controls on northern high latitude snow–albedo feedback: observations and CMIP5 model simulations. *Glob. Change Biol.* **20**, 594–606 (2014).
72. Myers-Smith, I. H. & Hik, D. S. Shrub canopies influence soil temperatures but not nutrient dynamics: an experimental test of tundra snow–shrub interactions. *Ecol. Evol.* **3**, 3683–3700 (2013).
73. DeMarco, J., Mack, M. C. & Bret-Harte, M. S. Effects of arctic shrub expansion on biophysical vs. biogeochemical drivers of litter decomposition. *Ecology* **95**, 1861–1875 (2014).
74. Enquist, B. J., Brown, J. H. & West, G. B. Allometric scaling of plant energetics and population density. *Nature* **395**, 163–165 (1998).
75. Street, L. E., Shaver, G. R., Williams, M. & van Wijk, M. T. What is the relationship between changes in canopy leaf area and changes in photosynthetic CO_2 flux in arctic ecosystems? *J. Ecol.* **95**, 139–150 (2007).
76. Poorter, H. et al. Biomass allocation to leaves, stems and roots: meta-analyses of interspecific variation and environmental control. *New Phytol.* **193**, 30–50 (2012).
77. Greaves, H. E. et al. Estimating aboveground biomass and leaf area of low-stature Arctic shrubs with terrestrial LiDAR. *Remote Sens. Environ.* **164**, 26–35 (2015).
78. Westoby, M. & Wright, I. J. Land-plant ecology on the basis of functional traits. *Trends Ecol. Evol.* **21**, 261–268 (2006).
79. Niinemets, Ü. A review of light interception in plant stands from leaf to canopy in different plant functional types and in species with varying shade tolerance. *Ecol. Res.* **25**, 693–714 (2010).
80. Freschet, G. T., Aerts, R. & Cornelissen, J. H. C. A plant economics spectrum of litter decomposability. *Funct. Ecol.* **26**, 56–65 (2012).
81. Manning, P. et al. Simple measures of climate, soil properties and plant traits predict national-scale grassland soil carbon stocks. *J. Appl. Ecol.* **52**, 1188–1196 (2015).
82. Iida, Y. et al. Wood density explains architectural differentiation across 145 co-occurring tropical tree species. *Funct. Ecol.* **26**, 274–282 (2012).
83. Ménard, C. B., Essery, R., Pomeroy, J., Marsh, P. & Clark, D. B. A shrub bending model to calculate the albedo of shrub-tundra. *Hydrol. Processes* **28**, 341–351 (2014).
84. Nauta, A. L. et al. Permafrost collapse after shrub removal shifts tundra ecosystem to a methane source. *Nat. Clim. Change* **5**, 67–70 (2015).
85. Hobbie, S. E. Temperature and plant species control over litter decomposition in Alaskan tundra. *Ecol. Monogr.* **66**, 503–522 (1996).
86. Weedon, J. T. et al. Global meta-analysis of wood decomposition rates: a role for trait variation among tree species? *Ecol. Lett.* **12**, 45–56 (2009).
87. Dorrepaal, E., Cornelissen, J., Aerts, R., Wallen, B. & van Logtestijn, R. Are growth forms consistent predictors of leaf litter quality and decomposability across peatlands along a latitudinal gradient? *J. Ecol.* **93**, 817–828 (2005).
88. Larsen, K. S., Michelsen, A., Jonasson, S., Beier, C. & Grogan, P. Nitrogen uptake during fall, winter and spring differs among plant functional groups in a subarctic heath ecosystem. *Ecosystems* **15**, 927–939 (2012).
89. Chapin, F. S. III, Shaver, G. R., Giblin, A. E., Nadelhoffer, K. J. & Laundre, J. A. Responses of arctic tundra to experimental and observed changes in climate. *Ecology* **76**, 694–711 (1995).
90. Reich, P. B., Walters, M. B. & Ellsworth, D. S. From tropics to tundra: global convergence in plant functioning. *Proc. Natl Acad. Sci. USA* **94**, 13730–13734 (1997).

© 2018 Springer Nature Limited. All rights reserved.

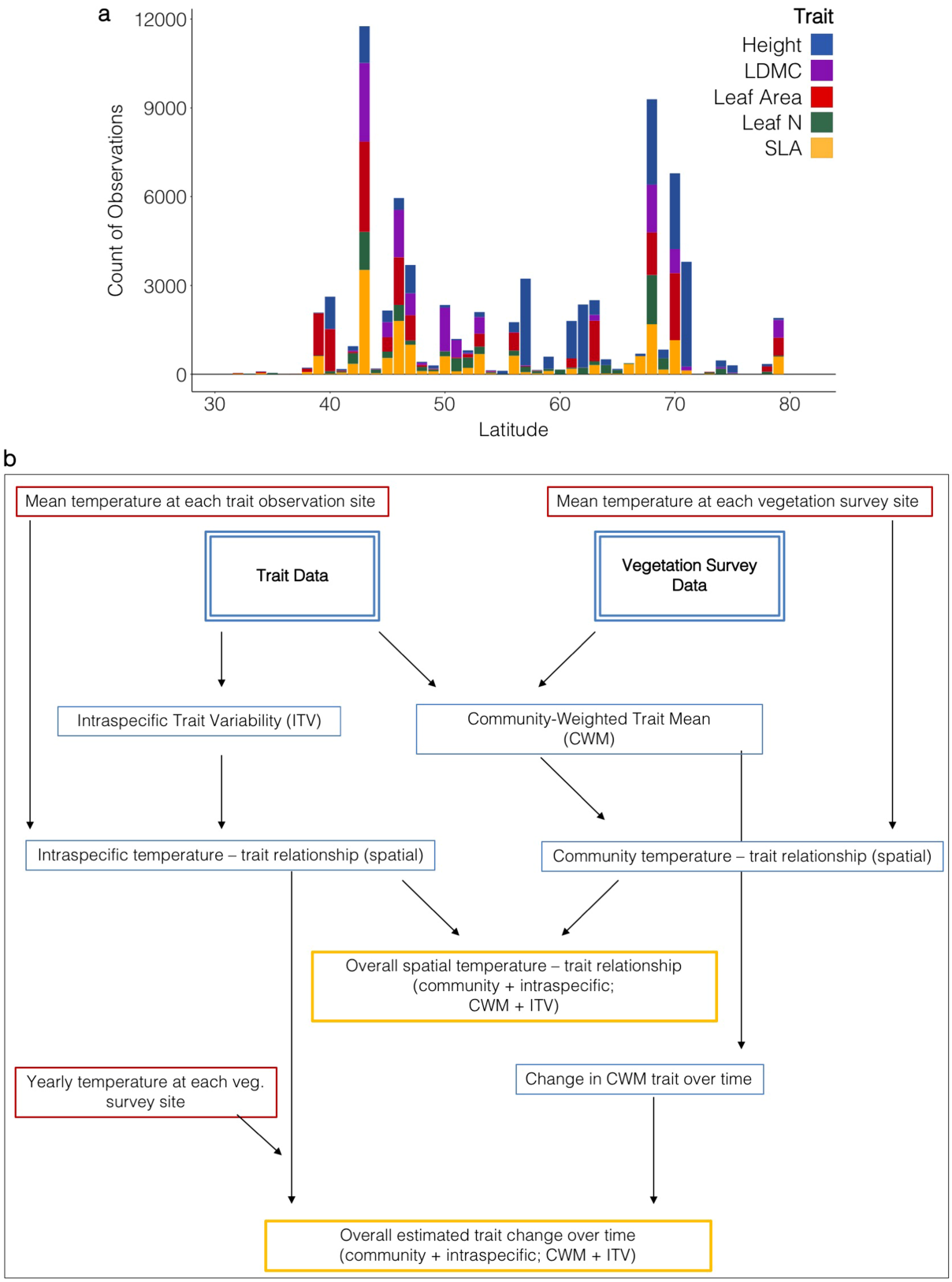

Extended Data Fig. 1 | Overview of trait data and analyses. a, Count of traits per latitude (rounded to the nearest degree) for all georeferenced observations in TRY and TTT that correspond to species in the vegetation survey dataset. **b**, Work flow and analyses of temperature–trait relationships. Intraspecific temperature–trait relationships over space were used to estimate the potential contribution of ITV to overall temperature–trait relationships over space and time (CWM + ITV) as trait measurements for individual plants over time are not available.

© 2018 Springer Nature Limited. All rights reserved.

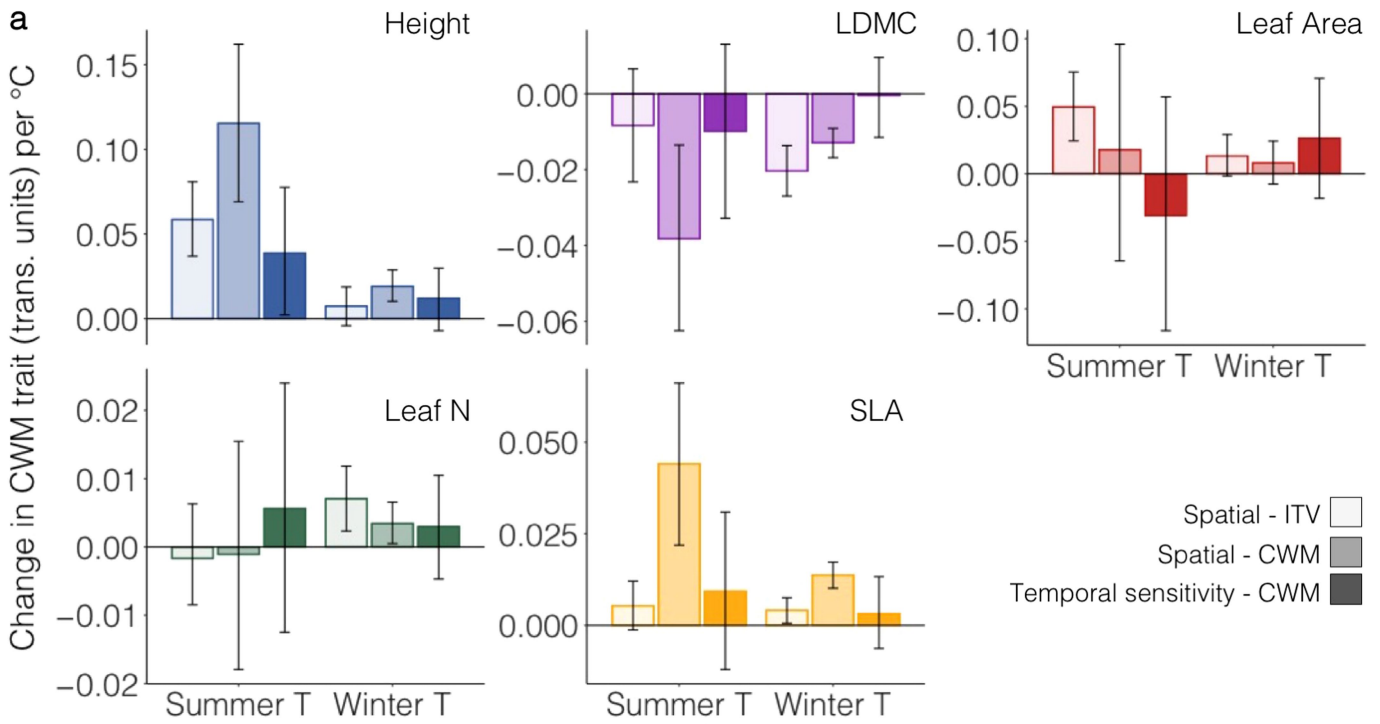

Extended Data Fig. 2 | All temperature–trait relationships. Slope of temperature–trait relationships over space (within-species (ITV) and across communities (CWM)) and with interannual variation in temperature (community temperature sensitivity). Spatial - ITV, spatial relationship between ITV and temperature; spatial-CWM, spatial relationship between CWM and summer temperature; temporal sensitivity-CWM, temperature sensitivity of CWM (that is, correspondence between interannual variation in CWM values with interannual variation in temperature). Error bars represent 95% credible intervals on the slope estimate. We used five-year mean temperatures (temperature of the survey year and four previous years) to estimate temperature sensitivity, because this interval has been shown to explain vegetation change in tundra[20] and alpine[29] plant communities. All slope estimates are in transformed units (height = log(cm), LDMC = logit(g g^{-1}), leaf area = log(cm^2), leaf nitrogen = log(mg g^{-1}), SLA = log(mm^2 mg^{-1})). Community (CWM) temperature–trait relationships are estimated across all 117 sites; intraspecific temperature–trait relationships are estimated as the mean of 108 and 109 species for SLA, 80 and 86 species for plant height, 74 and 72 species for leaf nitrogen, 85 and 76 species for leaf area, and 43 and 52 species for LDMC, for summer and winter temperature, respectively (see Methods for details).

© 2018 Springer Nature Limited. All rights reserved.

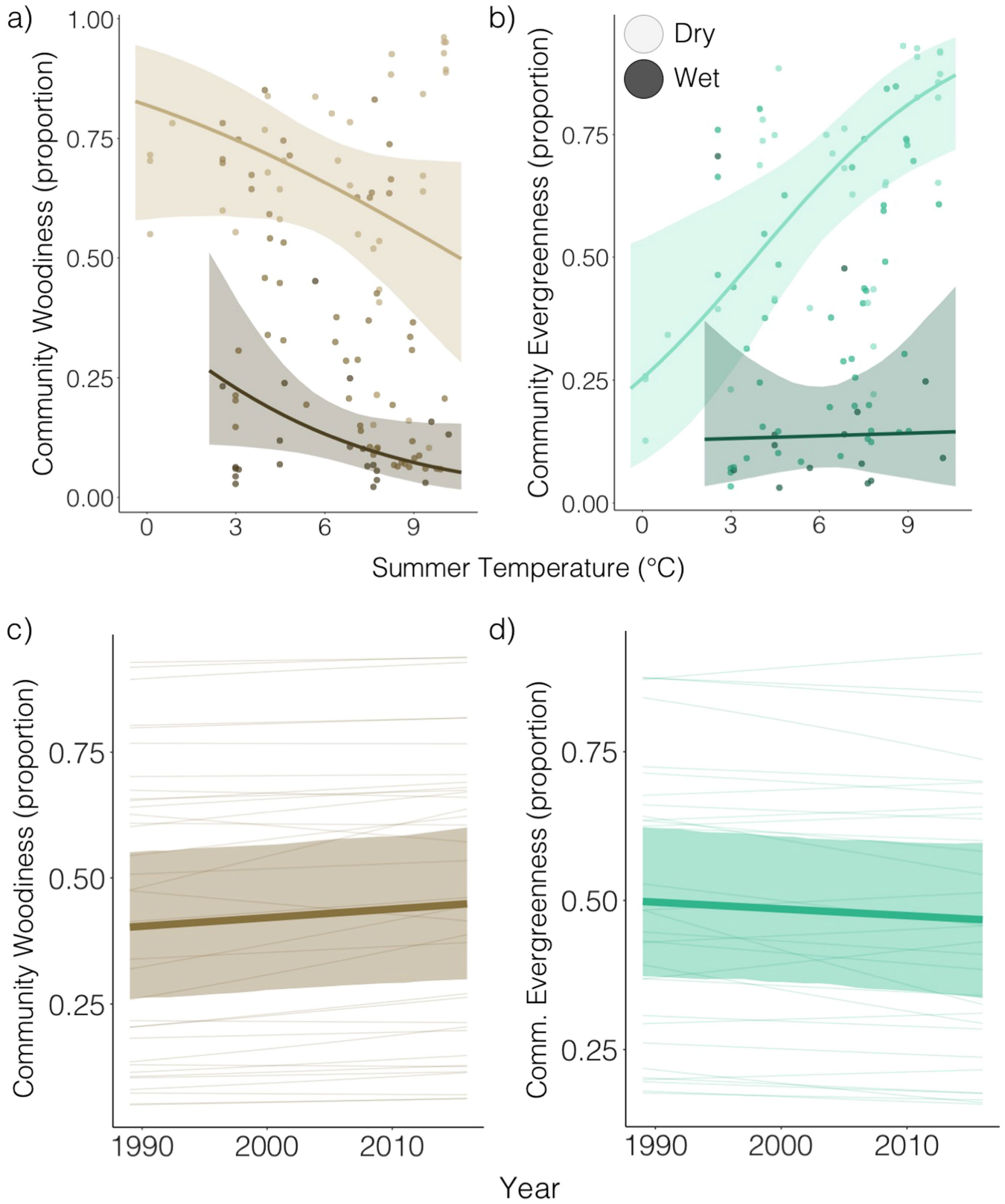

Extended Data Fig. 3 | See next page for caption.

© 2018 Springer Nature Limited. All rights reserved.

Extended Data Fig. 3 | Community woodiness and evergreenness over space and time. a, **b**, Variation in community woodiness (**a**) and evergreenness (**b**) across space with summer temperature and soil moisture. Community woodiness is the abundance-weighted proportion of woody species versus all other plant species in the community. Community evergreenness is the abundance-weighted proportion of evergreen shrubs versus all shrub species (deciduous and evergreen). The evergreen model was generated using a reduced number of sites (98 instead of 117), because some sites did not have any woody species (and it was thus not possible to calculate a proportion of evergreen species). Both temperature and moisture were important predictors of community woodiness and evergreenness. The 95% credible interval for a temperature × moisture interaction term overlapped zero in both models (−0.100 to 0.114 and −0.201 to 0.069 for woodiness and evergreenness, respectively). **c**, **d**, There was no change over time in woodiness (**c**) or evergreenness (**d**). Thin lines represent slopes per site (woodiness, $n = 117$ sites; evergreenness, $n = 98$ sites). In all panels, bold lines indicate overall model predictions and shaded ribbons designate 95% credible intervals on these model predictions.

© 2018 Springer Nature Limited. All rights reserved.

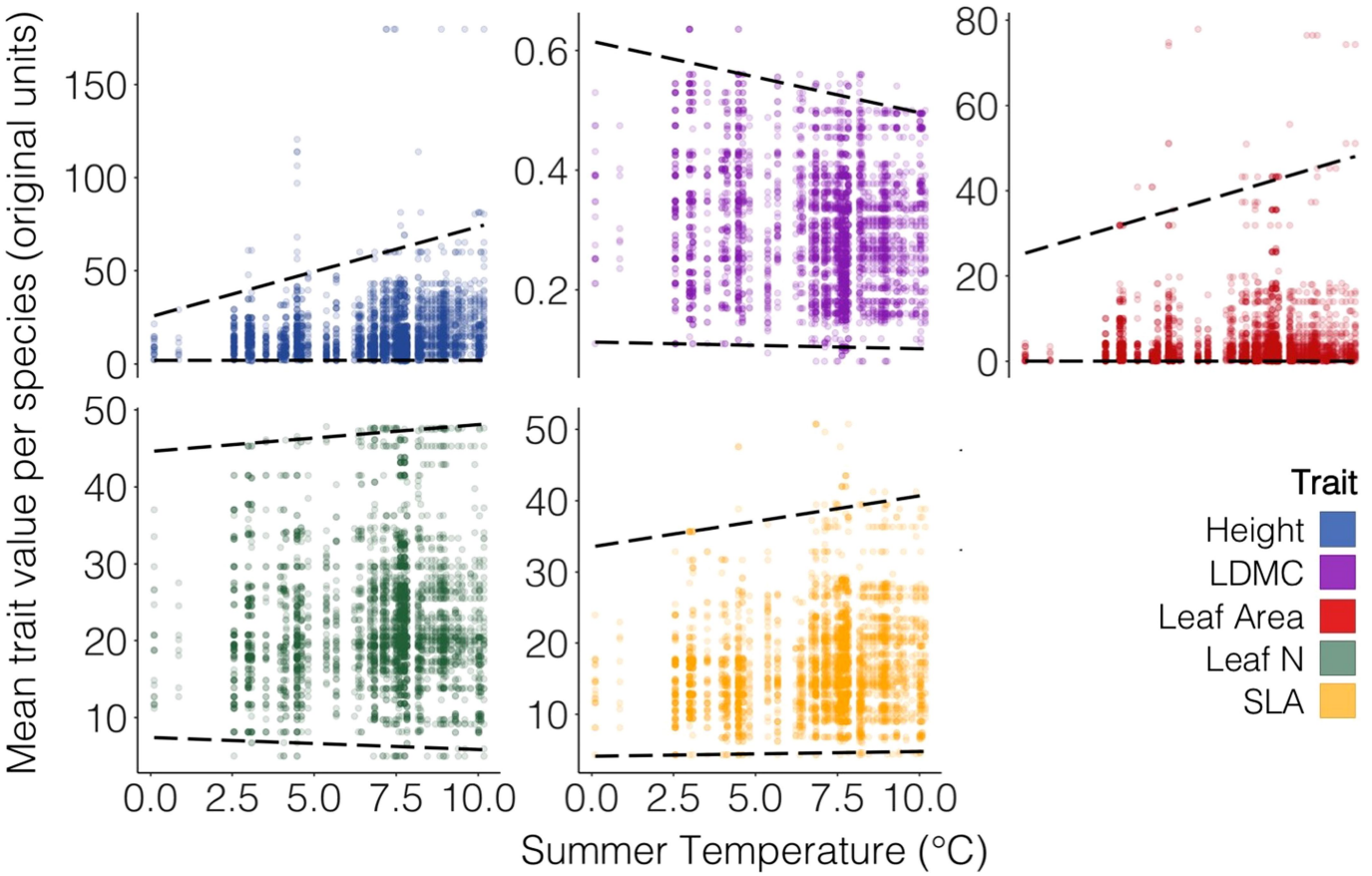

Extended Data Fig. 4 | Range in species mean values of each trait by summer temperature. Black dashed lines represent quantile regression estimates for 1% and 99% quantiles. Species mean values are estimated from intercept-only Bayesian models using the estimation technique described in the Methods (see 'Calculation of CWM values'). Species locations are based on species in the 117 vegetation survey sites. All values are back-transformed into their original units (height (cm), LDMC ($g\ g^{-1}$), leaf area (cm^2), leaf nitrogen ($mg\ g^{-1}$), SLA ($mm^2\ mg^{-1}$).

© 2018 Springer Nature Limited. All rights reserved.

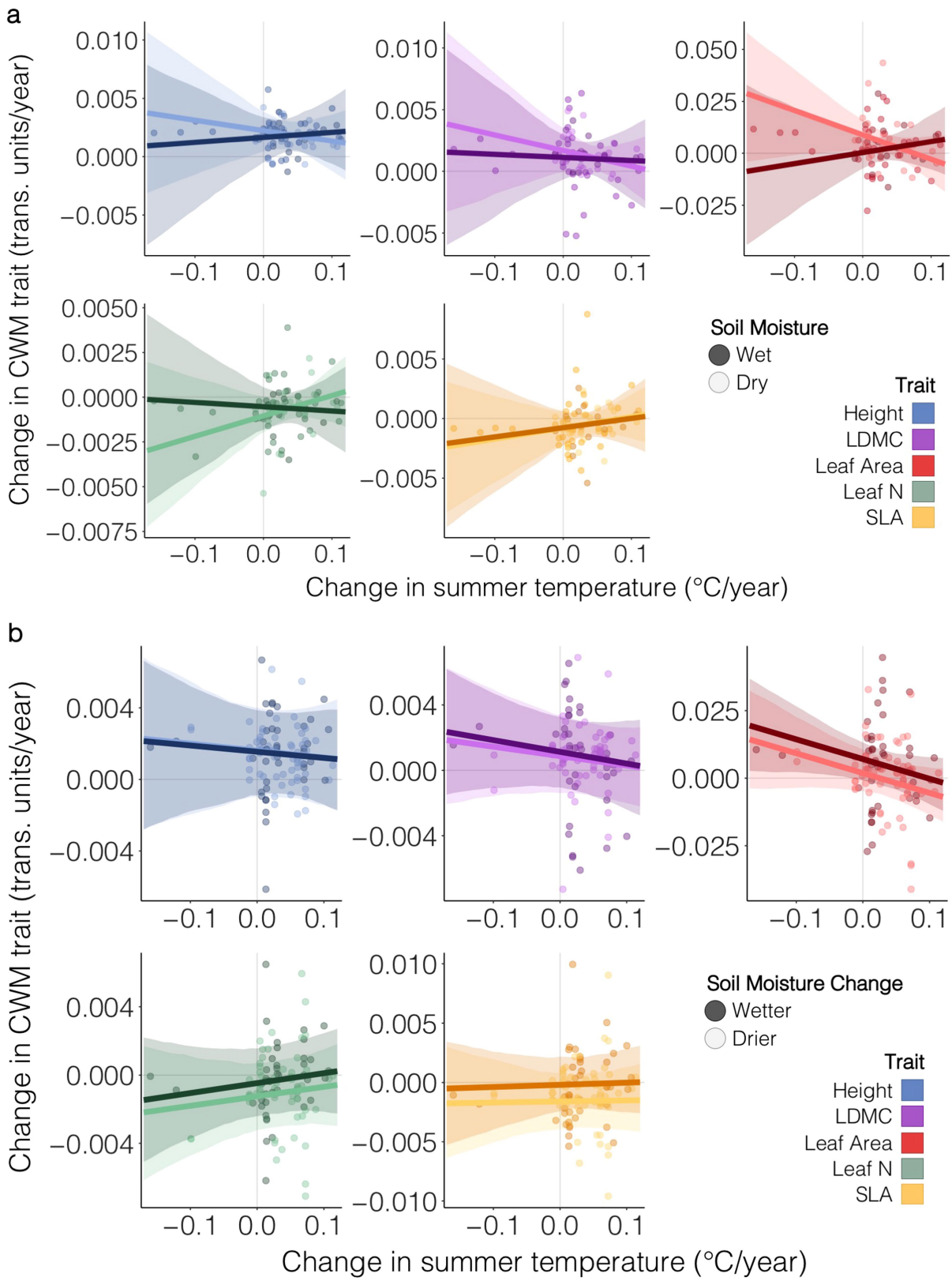

Extended Data Fig. 5 | The rate of community trait change is not related to the rate of temperature change or soil moisture for any trait. a, **b**, Rate of CWM change over time per site ($n = 117$ sites) related to temperature change and long-term mean soil moisture (**a**) or soil moisture change (**b**) at a site. Points represent mean trait change values for each site, lines represent the predicted relationship between trait change, temperature change and soil moisture or soil moisture change, and transparent ribbons are the 95% credible intervals on these predictions. Both mean soil moisture and soil moisture change were modelled as a continuous variables, but are shown as predictions for minimum and maximum values or rates of change. Trait change estimates are in transformed units (log for height, leaf area, leaf nitrogen and SLA, and logit for LDMC). Soil moisture change was estimated from downscaled ERA-Interim data and may not accurately represent local changes in moisture availability at each site.

© 2018 Springer Nature Limited. All rights reserved.

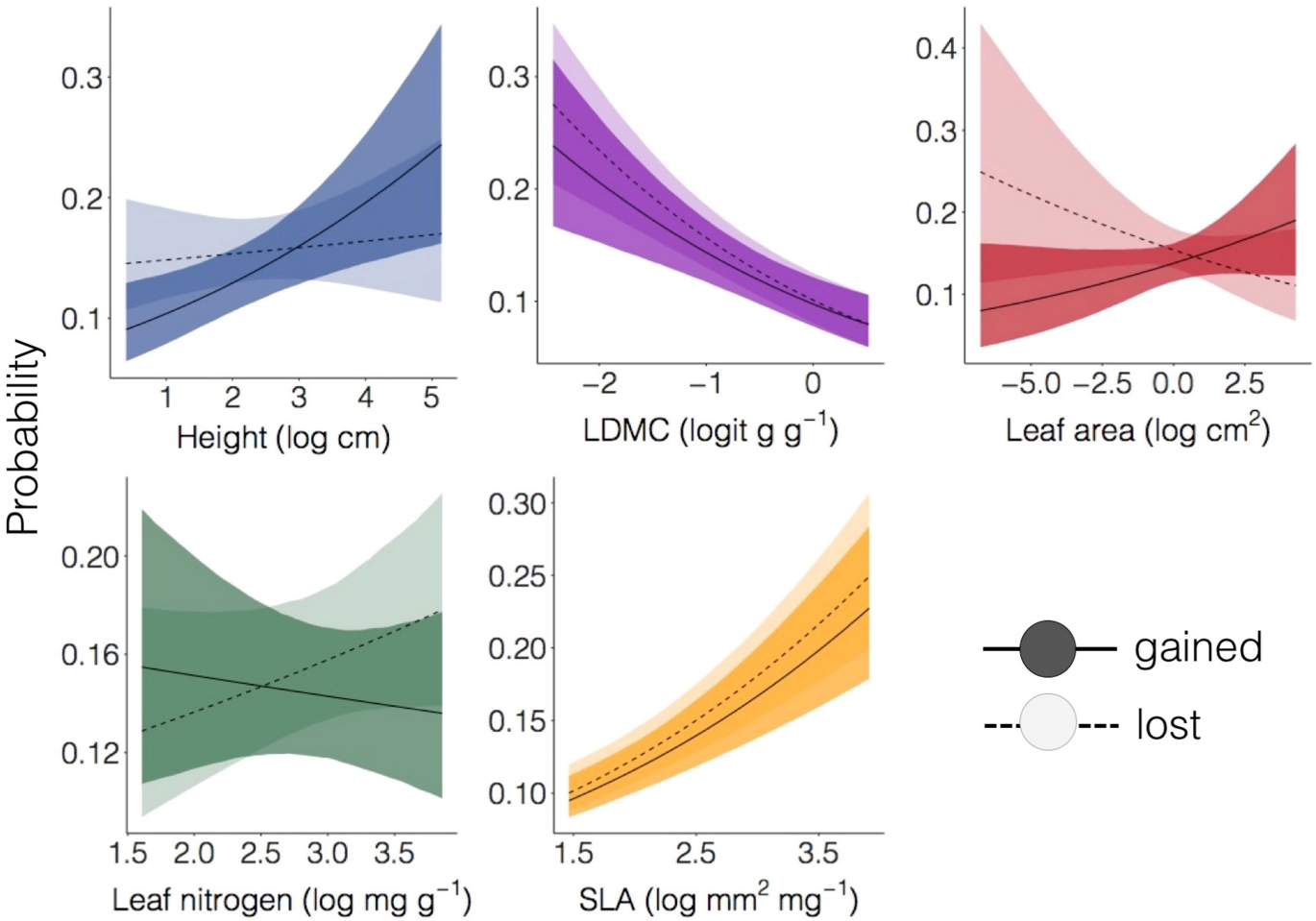

Extended Data Fig. 6 | Increasing community height is driven by the immigration of taller species, not the loss of shorter ones. Probability that a species newly arrived in a site (gained) or disappeared from a site (lost) as a function of its traits ($n = 117$ sites). Lines and ribbons represent overall model predictions and the 95% credible intervals on these predictions, respectively. Dark ribbons and solid lines represent species gains whereas pale ribbons and dashed lines represent species losses. Only for plant height was the trait–probability relationship different for gains and losses.

© 2018 Springer Nature Limited. All rights reserved.

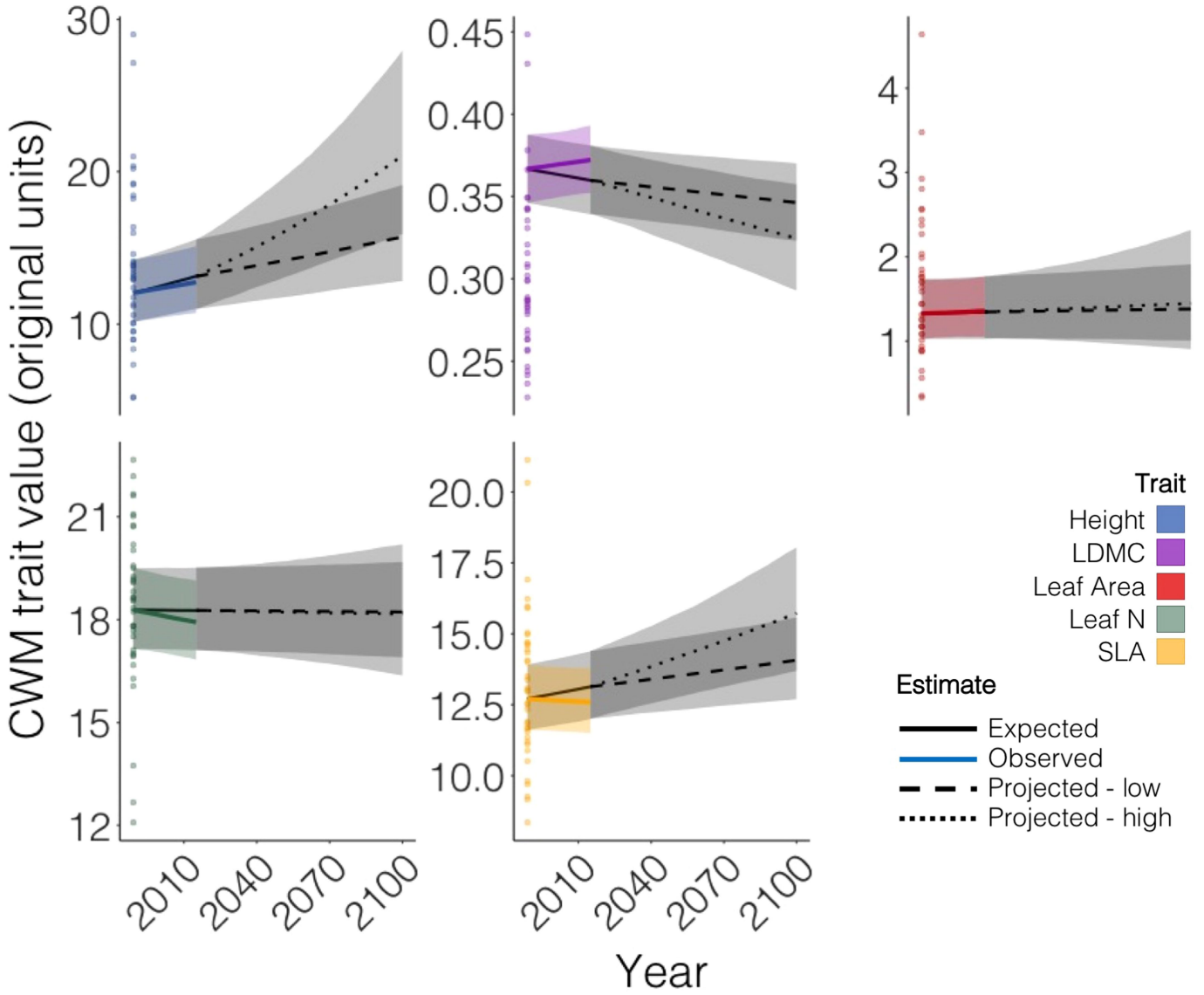

Extended Data Fig. 7 | Comparison of actual, expected and projected CWM trait change over time. Actual, expected and projected CWM trait changes are shown as solid coloured, solid black, and dashed or dotted lines, respectively. The expected trait change is calculated using the observed spatial temperature–trait relationship and the average rate of recent summer warming across all sites. Note that these projections assume no change in soil moisture conditions. The dotted and dashed black lines after 2015 show the projected trait change for the maximum (RCP8.5) and minimum (RCP2.6) IPCC carbon emission scenarios, respectively, from the HadGEM2 AO Global Circulation Model, given the expected temperature change associated with those scenarios. Points along the left axis of each panel show the distribution of present-day CWM per site ($n = 117$ sites) to better demonstrate the magnitude of projected change. Values are in original units (height (cm), LDMC ($g\ g^{-1}$), leaf area (cm^2), leaf nitrogen ($mg\ g^{-1}$) and SLA ($mm^2\ mg^{-1}$)).

© 2018 Springer Nature Limited. All rights reserved.

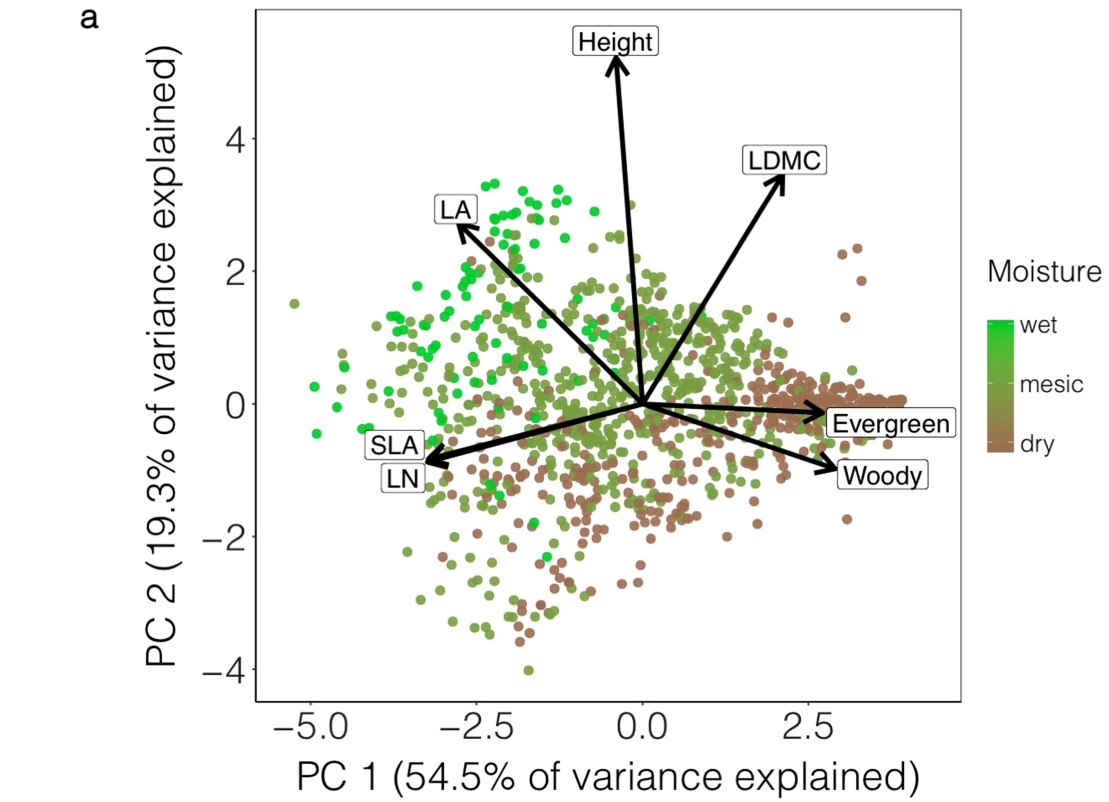

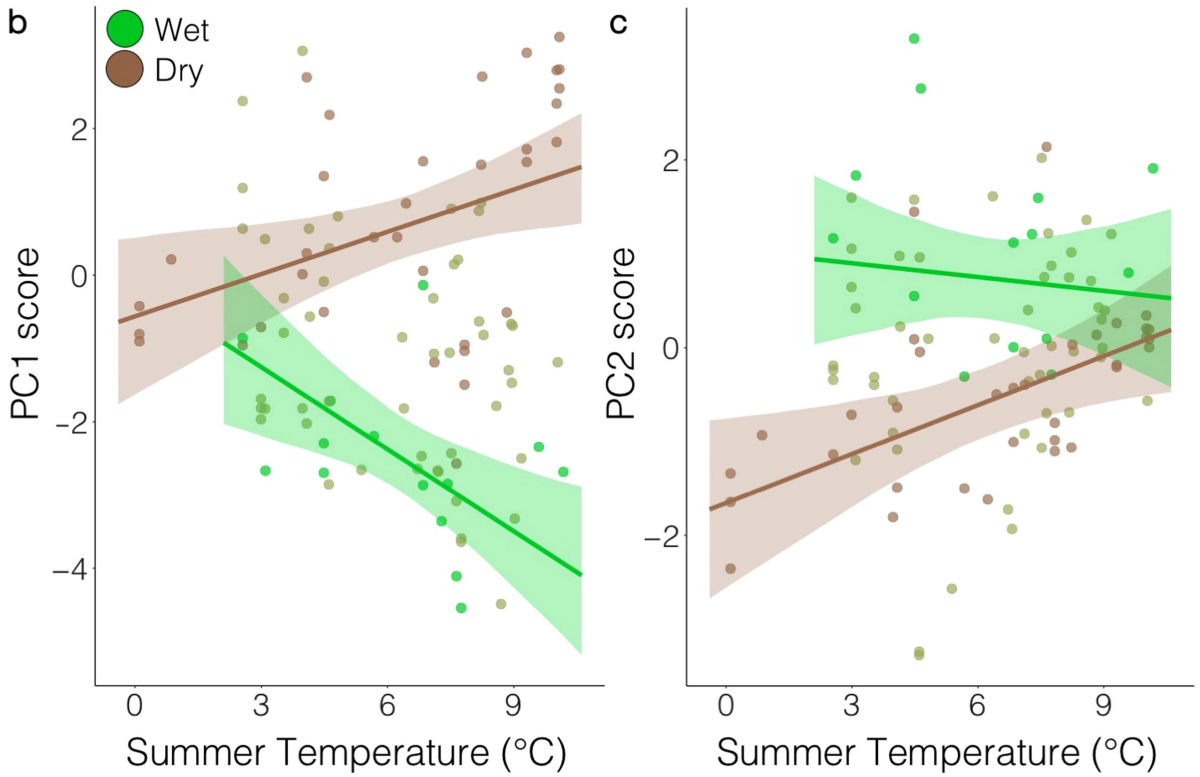

Extended Data Fig. 8 | Community trait co-variation is structured by temperature and moisture. a, PCA of plot-level community-weighted traits for seven key functional traits demonstrating how communities vary in multidimensional trait space. Trait correlations are highest between SLA and leaf nitrogen, and evergreenness and woodiness. Variation in SLA, leaf nitrogen, evergreenness and woodiness (principal component (PC)1) are orthogonal to variation in height (PC2). Variation in leaf area and LDMC are explained by both PC1 and PC2. The colour of the points indicates the soil moisture status of each plot at the site-level. **b**, **c**, Plot scores along PC1, related to plant resource economy, vary with summer temperature, soil moisture and their interaction (**b**), whereas plot scores along PC2 vary only with soil moisture (**c**). The colour of the points indicates the soil moisture of each site. Because not all plots and sites had woody species (and thus proportion evergreen could not be calculated), this analysis was conducted on a subset of 1,098 (out of 1,520) plots at 98 (out of 117) different sites.

© 2018 Springer Nature Limited. All rights reserved.

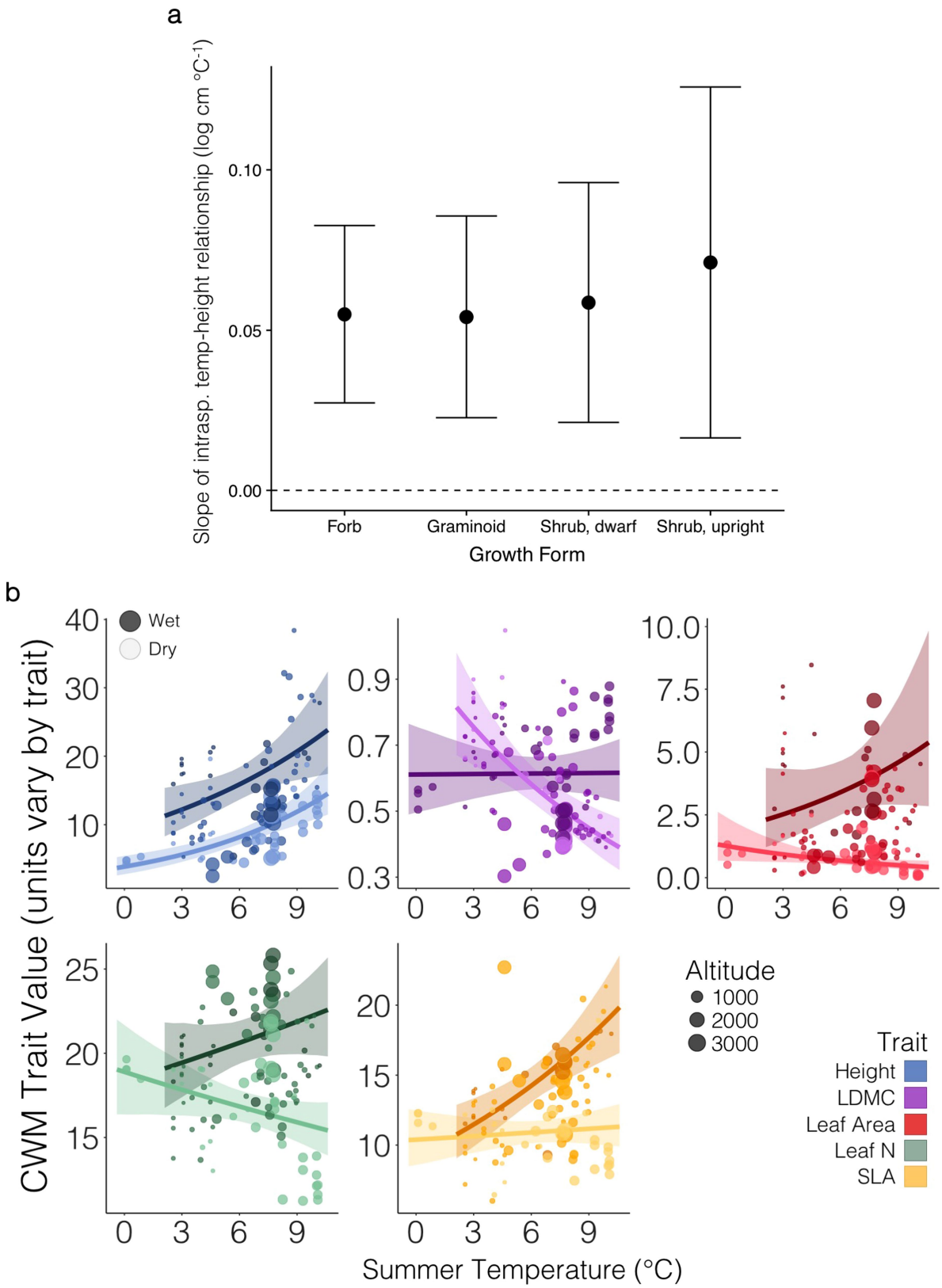

Extended Data Fig. 9 | Temperature–trait relationships by growth form and site elevation. a, Mean (±s.d.) intraspecific temperature–height relationships ($n = 80$ species) per functional group. Dwarf shrubs are defined as those shrubs that do not grow above 30 cm in height (as estimated by regional floras, such as Flora of North America, USDA or the Royal Horticultural Society) and are generally genetically limited in their ability to grow upright. There are no differences among functional groups in the magnitude of mean intraspecific temperature–height relationships. **b**, Relationship between community-weighted trait values, summer temperature and soil moisture across biogeographical gradients, as in Fig. 2a. Points represent mean estimates per site ($n = 117$ sites) and are sized by the elevation of the site (larger circles indicate higher elevation). Ribbons represent the overall trait–temperature–moisture relationship (95% credible intervals on predictions at minimum and maximum soil moisture) across all sites.

© 2018 Springer Nature Limited. All rights reserved.

Extended Data Table 1 | Ecosystem functions influenced by each of the seven plant traits

Ecosystem function	Example references
Plant Height	
Above ground biomass	Chapin et al., 1996[61]; Weiher et al., 1999[62]; Lavorel and Garnier, 2002[6]; Violle et al., 2007[63]; Hudson and Henry, 2009[64]
Carbon stock	Lavorel and Garnier, 2002[6]; De Deyn et al., 2008[65]; Moles et al., 2009[14]; Sistla et al., 2013[3]
Light Capture	Moles et al., 2009[14]
Competition	Lavorel and Garnier, 2002[6]; Kunstler et al., 2016[66]
Seed dispersal	Gaudet and Keddy, 1988[67]; Westoby et al., 2002[68]; Moles et al., 2009[14]; Moles & Leishman 2008[69]
Albedo	Sturm et al., 2001[70]; Sturm and Douglas, 2005[12]; Loranty et al., 2014[71]
Snow cover	Sturm et al., 2001[70]; Myers-Smith and Hik, 2013[72]; DeMarco et al., 2014[73]
Disturbance response	Lavorel and Garnier, 2002[6]
Max. population density	Enquist et al. 1998[74]
Leaf Area	
Above ground biomass	Street et al., 2007[75]; Poorter et al., 2012[76]; Greaves et al., 2015[77]
Albedo	Westoby and Wright, 2006[78]
Light interception	Niinemets, 2010[79]; Díaz et al., 2016[17]
Leaf water balance	Díaz et al., 2016[17]
Leaf energy balance	Díaz et al., 2016[17]
Specific Leaf Area	
Relative growth rate	Weiher et al., 1999[62]; Wright et al., 2004[8]; Reich, 2014[37]
Decomposition	Lavorel and Garnier, 2002[6]; Díaz et al., 2004[9]; Cornelissen et al., 2007[5]; Cornwell et al., 2008[10]; Freschet et al., 2012[80]
Leaf life span	Reich, 2014[37]; Wright et al., 2004[8]; Diaz et al., 2004[9]
Leaf Nitrogen	
Decomposition	Lavorel and Garnier, 2002[6]; Cornelissen et al., 2007[5]; Cornwell et al., 2008[10]; Freschet et al., 2012[80]
Primary productivity	Weiher et al., 1999[62]; Wright et al., 2004[8]; Reich, 2014[37]
Soil carbon stocks	Manning et al., 2015[81]
Leaf Dry Matter Content	
Decomposition	Lavorel and Garnier, 2002[6]; Cornelissen et al., 2007[5]; Cornwell et al., 2008[10]; Freschet et al., 2012[80]
Soil carbon stocks	Manning et al., 2015[81]
Woodiness	
Plant architecture	Chapin et al., 1996[61]; Lida et al., 2012[82]
Albedo	Sturm et al., 2001[70]; Ménard et al., 2014[83])
Thermal insulation	Blok et al., 2010[30]; Myers-Smith and Hik, 2013[72]; Nauta et al., 2014[84]
Decomposition	Hobbie, 1996[85]; Cornelissen et al., 2007[5]; Weedon et al., 2009[86]
Carbon storage	Hobbie, 1996[85]; Myers-Smith et al., 2011[11]; Sistla et al., 2013[3]
Evergreenness	
Decomposition	Dorrepaal et al., 2005[87]; Cornelissen et al., 2007[5]; Cornwell et al., 2008[10]
Nutrient cycling	Larsen et al., 2012[88]
Relative growth rate	Chapin et al., 1995[89]; Reich et al., 1997[90]

Data are from previous publications[61–90].

© 2018 Springer Nature Limited. All rights reserved.

nature research

Corresponding author(s): Anne D. Bjorkman

Reporting Summary

Nature Research wishes to improve the reproducibility of the work that we publish. This form provides structure for consistency and transparency in reporting. For further information on Nature Research policies, see Authors & Referees and the Editorial Policy Checklist.

Statistical parameters

When statistical analyses are reported, confirm that the following items are present in the relevant location (e.g. figure legend, table legend, main text, or Methods section).

n/a	Confirmed	
☐	☒	The exact sample size (*n*) for each experimental group/condition, given as a discrete number and unit of measurement
☐	☒	An indication of whether measurements were taken from distinct samples or whether the same sample was measured repeatedly
☐	☒	The statistical test(s) used AND whether they are one- or two-sided *Only common tests should be described solely by name; describe more complex techniques in the Methods section.*
☐	☒	A description of all covariates tested
☐	☒	A description of any assumptions or corrections, such as tests of normality and adjustment for multiple comparisons
☐	☒	A full description of the statistics including central tendency (e.g. means) or other basic estimates (e.g. regression coefficient) AND variation (e.g. standard deviation) or associated estimates of uncertainty (e.g. confidence intervals)
☒	☐	For null hypothesis testing, the test statistic (e.g. *F*, *t*, *r*) with confidence intervals, effect sizes, degrees of freedom and *P* value noted *Give P values as exact values whenever suitable.*
☐	☒	For Bayesian analysis, information on the choice of priors and Markov chain Monte Carlo settings
☐	☒	For hierarchical and complex designs, identification of the appropriate level for tests and full reporting of outcomes
☐	☒	Estimates of effect sizes (e.g. Cohen's *d*, Pearson's *r*), indicating how they were calculated
☐	☒	Clearly defined error bars *State explicitly what error bars represent (e.g. SD, SE, CI)*

Our web collection on statistics for biologists may be useful.

Software and code

Policy information about availability of computer code

Data collection	No software or code was used in the collection of community composition data. Trait data come from a variety of sources and information about software used is often not available. In some cases, ImageJ (various versions) was used to estimate leaf area.
Data analysis	All Bayesian analyses were done in either JAGS or Stan through R (v. 3.3.3) using the packages rjags (v. 4.6) or rstan (v2.14.1). The R package Taxonstand (v. 1.8) was used to clean species names and identify synonyms. The R package vegan (v. 2.4.6) was used in the ordination. All graphs were made using the R package ggplot2 (2009). Model equations are provided in the methods for all analyses. Model code (Stan) is provided for the two main analyses in the supplementary information.

For manuscripts utilizing custom algorithms or software that are central to the research but not yet described in published literature, software must be made available to editors/reviewers upon request. We strongly encourage code deposition in a community repository (e.g. GitHub). See the Nature Research guidelines for submitting code & software for further information.

Data

Policy information about availability of data

All manuscripts must include a data availability statement. This statement should provide the following information, where applicable:

- Accession codes, unique identifiers, or web links for publicly available datasets
- A list of figures that have associated raw data
- A description of any restrictions on data availability

Trait data
Data compiled through the Tundra Trait Team are publicly accessible (see data paper published in Global Ecology & Biogeography; Bjorkman et al. in press). The public TTT database includes traits not considered in this study as well as tundra species that do not occur in our vegetation survey plots, for a total of nearly 92,000 trait observations on 978 species. Additional trait data from the TRY trait database can be requested at try-db.org.

Composition data
Most sites and years of the vegetation survey data included in this study are available in the Polar Data Catalogue (ID # 10786_iso). Much of the individual site-level data has additionally been made available in the BioTIME database (Dornelas et al. 2018; https://synergy.st-andrews.ac.uk/biotime/biotime-database/).

References
Bjorkman, AD, IH Myers-Smith, SC Elmendorf, S Normand, HJD Thomas, et al. Tundra Trait Team: a database of plant traits spanning the tundra biome. Global Ecology and Biogeography. In press.
Dornelas, M, LH Antão, F Moyes, AE Bates, AE Magurran, et al. 2018. BioTIME: A database of biodiversity time series for the Anthropocene. Global Ecology and Biogeography. 27: 760-786.

Field-specific reporting

Please select the best fit for your research. If you are not sure, read the appropriate sections before making your selection.

☐ Life sciences ☐ Behavioural & social sciences ☒ Ecological, evolutionary & environmental sciences

For a reference copy of the document with all sections, see nature.com/authors/policies/ReportingSummary-flat.pdf

Ecological, evolutionary & environmental sciences study design

All studies must disclose on these points even when the disclosure is negative.

Study description	The study involves plant community composition data at 117 sites around the Northern Hemisphere tundra biome. We used Bayesian hierarchical models for most analyses (plots nested within sites nested within regions). A region was defined as a WorldClim or CRU grid cell, depending on the analysis (across space or over time). We combined the community composition data with >50,000 trait observations from the TRY and TTT trait databases.
Research sample	We focused on vascular plant species as trait data are rarely available for bryophytes. Most repeat vegetation sampling occurred in permanent marked plots (2/3) while the remainder were randomly placed plots within a specific area. Most of the community composition data was previously archived at the Polar Data Catalogue (ID # 10786_iso); trait data are available through the TTT (fully public) and TRY (partially public) trait databases.
Sampling strategy	We included all available community composition and functional trait data. Thus, sample size was not predetermined but rather a maximum possible based on available data.
Data collection	Data was collected by many different people in many different locations (see authorship contribution statement).
Timing and spatial scale	Community composition data were collected between 1989 and 2015 at 117 tundra sites, including Arctic tundra sites in Alaska, Canada, Fennoscandia, Iceland, and Siberia, and alpine tundra sites in the Colorado Rockies and European Alps. The exact sampling dates vary by site. Trait data were collected between 1964 and 2016 (though the vast majority of trait data were collected since the 1990's).
Data exclusions	In order to ensure that comparisons among sites are not biased due to the method of vegetation survey, we included only sites which were surveyed using a method equivalent to percent cover. Trait data were "cleaned" - first by removing any impossible values (e.g., LDMC values greater than 1, plant height of 0) and then according to the algorithm described in the methods. The trait data cleaning code, along with the cleaned and uncleaned versions of the trait dataset, are publicly available as a GitHub repository (see Bjorkman et al. Global Ecology and Biogeography, in press).
Reproducibility	Our study was not experimental, but the large number of sampling sites (117) spread across the Northern Hemisphere tundra biome ensures good spatial replication.
Randomization	Our study does not include experiments, thus samples were not randomly allocated into experimental groups. We account for spatial and temporal non-independence of samples by using a hierarchical approach to analysis (plots nested within sites nested within regions).

Blinding: Group allocation was based on physical proximity only (plots within sites within regions). Vegetation surveys were not conducted with the goal of documenting trait change over time, thus bias in data collection is unlikely.

Did the study involve field work? ☒ Yes ☐ No

Field work, collection and transport

Field conditions: Field conditions varied by site. All sites from which community composition data were collected have mean summer (warmest quarter) temperatures of 10 degrees C or less.

Location: Community composition data were collected in 117 tundra sites spanning the Northern Hemisphere (including both Arctic and alpine tundra). Trait data were collected in hundreds of locations across the Northern Hemisphere.

Access and import/export: The appropriate data collection permits were obtained whenever necessary. The permits necessary varied among the different sites.

Disturbance: Vegetation sampling was non-destructive. In some cases, trait measurements required removing between 1 and 10 leaves from an individual plant.

Reporting for specific materials, systems and methods

Materials & experimental systems

n/a	Involved in the study
☒	☐ Unique biological materials
☒	☐ Antibodies
☒	☐ Eukaryotic cell lines
☒	☐ Palaeontology
☒	☐ Animals and other organisms
☒	☐ Human research participants

Methods

n/a	Involved in the study
☒	☐ ChIP-seq
☒	☐ Flow cytometry
☒	☐ MRI-based neuroimaging